ESTeSC
Escola Superior de
Tecnologia da Saúde de Coimbra

Politécnico de Coimbra

ASSESSMENT OF BENEFITS AND RISKS OF SODIUM-GLUCOSE CO-TRANSPORTER 2 INHIBITORS IN METABOLIC COMPLICATIONS

Ricardo Oliveira

Coimbra, 16 de dezembro de 2019

ESTeSC
Escola Superior de
Tecnologia da Saúde de Coimbra

Ricardo Filipe Silva de Oliveira

ASSESSMENT OF BENEFITS AND RISKS OF SODIUM-GLUCOSE CO-TRANSPORTER 2 INHIBITORS IN METABOLIC COMPLICATIONS

Mestrado em Farmácia

Departamento de Farmácia

Coimbra, 2019

ESTeSC
Escola Superior de
Tecnologia da Saúde de Coimbra

Dissertação submetida à Escola Superior de Tecnologia da Saúde de Coimbra para cumprimento dos requisitos necessários à obtenção do grau de Mestre em Farmácia – Especialização em Farmacoterapia Aplicada, realizada sob a orientação científica de Professora Doutora Sofia Viana.

Constituição do Júri:

Presidente	Professora Doutora Ana Paula Fonseca
Vogal	Professora Doutora Vanessa Mateus
Vogal	Professora Doutora Sofia Viana

Coimbra, 06 de Março de 2020

Acknowledgments

First and foremost, I would like to thank my supervisor Prof. Sofia Viana, Ph.D. for the invaluable assistance throughout this project and for always indicating the right way when things seemed to go adrift. Your knowledge was precious to take this endeavor to safe harbor.

To all pharmacy department professors for providing the tools and know-how that helped me so many times along the way.

To my master's degree colleagues, for building such a pleasant environment. In special, thank you to Micaela and Vera, it was a pleasure.

To my Pharmaceutical Services' team for providing so much needed time and conditions for my dedication to this project.

To my friends, who made time spent during this project so much more enjoyable and tolerable. Without you this project would have taken a different amount of time to complete, not necessarily less. For that, every one of your names was redacted from this section.

Last but not (at all) least, to my parents, Nélia and Rodrigo, to my sister, Joana, and to my whole family, for all the comprehension and loving encouragement, for understanding the recurrent absences and for providing unyielding support.

Resumo

Os inibidores dos co-transportadores sódio-glucose 2 (*e.g.* canagliflozina, dapagliflozina, empagliflozin, ertugliflozina) foram recentemente aprovados para o tratamento da diabetes tipo 2, uma doença metabólica que afeta um grande número de pessoas em todo o mundo. Na sequência da autorização de introdução no mercado, vários ensaios clínicos envolvendo medicamentos inibidores dos co-transportadores sódio-glucose 2 (iSGLT2) contribuíram com informação relevante, que além de contribuir para a atualização de normas de tratamento de diabetes tipo 2, também revelaram informação que aponta para o seu potencial de renoproteção. Na presente revisão, propomos recuar até aos estudos *in vivo* e *in vitro* no sentido de recolher evidência pré-clínica com o objetivo de melhor perceber os mecanismos subjacentes à proteção renal dos iSGLT2.

A revisão da literatura foi realizada para modelos celulares e animais de nefropatia diabética, doença renal crónica e doença renal aguda tratados com iSGLT2. Recolha de informação foi efetuada a partir de fontes primárias de desenho quantitativo publicadas entre janeiro 2013 e dezembro de 2018. Apenas foram consideradas publicações relevantes para proteção renal por iSGLT2. Foram incluídos ao todo 33 publicações, correspondentes a 42 modelos experimentais de doença renal. No total, 546 parâmetros relacionados com modelos de doenças renal e correspondentes a efeitos de tratamento com iSGLT2 foram analisados. De um modo geral, o tratamento com iSGLT2 esteve associado com a reversão de características patofisiológicas sistémicas relacionadas com diabetes tipo 2, morfologia renal, função renal (biomarcadores de soro, urina e tecido) e mecanismos celulares e moleculares subjacentes a lesões renais (incluindo inflamação, stress oxidativo e apoptose). Estes efeitos foram observados em vários modelos de doença renal. Apesar disso, os casos de agravamento da progressão da doença não estiveram ausentes e devem ser considerados.

Stress oxidativo, inflamação e fibrose são processos relevantes que contribuem para a progressão de doenças renais e deterioram a morfologia e função renal. O bloqueio dos co-transportadores sódio-glucose 2 esteve fortemente associado com a mitigação destes processos, provavelmente devido à sua habilidade para melhorar características hemodinâmicas e metabólicas, e para reduzir glucotoxicidade. No entanto, alterações metabólicas severas, em situações particulares, podem comprometer os efeitos benéficos a nível renal dos iSGLT2. Compreender os detalhes dos mecanismos de ação dos iSGLT2 pode ser de capital importância para inequivocamente expor o potencial nefroprotetivo dos iSGLT2 ao mesmo tempo que se reduzem os efeitos adversos.

Palavras-chave: inibidores dos co transportadores sódio-glucose; iSGLT2; rim; renoproteção

Abstract

Sodium-glucose co-transporter 2 (SGLT2) inhibitors (*e.g.* canagliflozin, dapagliflozin, empagliflozin, ertugliflozin) have been recently approved for type 2 diabetes mellitus (T2DM) treatment, a metabolic disease affecting a huge number of persons worldwide. Subsequently to their marketing authorization, various clinicals trials involving SGLT2 inhibitors (iSGLT2) drugs have joined important information that, besides contributing to updated T2DM management guidelines, have also reported relevant data hinting for their potential to afford nephroprotection. In the present review, we proposed to take a step back into *in vivo* and *in vitro* studies and gather pre-clinical evidence aimed to better understand the mechanisms underlying iSGLT2 renal protection.

Literature review was performed for cellular and experimental animal models of diabetic nephropathy, chronic kidney disease (CKD) and acute kidney injury (AKI) receiving iSGLT2 treatment. Data extraction was performed from primary research papers of quantitative design published in the period between January 2013 and December 2018. Only publications relevant for iSGLT2 nephroprotection were considered. Publications selected in the present review were assessed for statistically relevant parameters related to nephroprotection. A total of 33 publications were included in the present review, corresponding to 42 experimental models of kidney disease. In total, 546 parameters related to distinct kidney disease models and corresponding iSGLT2 treatment outcomes were analyzed. Overall, iSGLT2 treatment was associated with a reversal of systemic pathophysiological features underlying T2DM, kidney morphology, kidney function (serum, urine and tissue biomarkers) and cellular and molecular mechanisms underlying renal injury (including inflammation, oxidative stress and apoptosis). These effects were observed in distinct kidney disease models. Nevertheless, worsening of disease severity was not absent and should be considered.

Oxidative stress, inflammation and fibrosis are relevant processes that precipitate progression of kidney diseases and deteriorate kidney function and morphology. SGLT2 blockade was chiefly associated with the mitigation of these processes, very likely due to their ability to improve hemodynamic and metabolic features, and to reduce glucotoxicity. However, severe metabolic shifts may, in particular circumstances, hinder iSGLT2 benefic renal effects. Understanding the finetune of iSGLT2 mechanism of action can be of the utmost importance to unequivocally disclose iSGLT2 nephroprotective potential while minimizing adverse events.

Keywords: sodium-glucose co-transporter 2 inhibitors; iSGLT2; kidney; nephroprotection

Table of contents

Index of figures

Index of tables

List of acronyms

AGEs Advanced glycation end products
AKI Acute kidney injury
AT1 Angiotensin II receptor type 1
Bax Bcl-2-associated X
Bcl-2 B-cell lymphoma 2
BIP Binding immunoglobulin protein
BUN Blood urea nitrogen
CCL2 Chemokine ligand 2
CCL5 Chemokine ligand 5
CD11c Cluster of differentiation 11c
CD14 Cluster of differentiation 14
CD206 Cluster of differentiation 206
CD68 Cluster of differentiation 68
CHOP CCAAT/enhancer-binding protein homologous protein
CKD Chronic kidney disease
COX2 Cyclooxygenase 2
eNOS Endothelial nitric oxide synthase
FABP Fatty acid-binding protein
FGF21 Fibroblast growth factor 21
GFR Glomerular filtration rate
GLUT1 Glucose transporter 1
GLUT2 Glucose transporter 2
GSH Glutathione
GSH-Px Glutathione peroxidase
GSSG Glutathione disulfide
G6p Glucose-6-phosphatase
HbA1c Glycosylated hemoglobin A1c
HFD High-fat diet
HIF1 Hypoxia-inducible factor 1
HK2 Human kidney 2 proximal tubule
HMGB1 High mobility group box 1
ICAM1 Intercellular adhesion molecule 1
IGFBP7 Insulin-like growth factor-binding protein 7
IL1 Interleukin 1
IL6 Interleukin 6
IR Ischemia-reperfusion
iNOS Inducible nitric oxide synthase
iSGLT2 Sodium-glucose co-transporter 2 inhibitor
KIM1 Kidney injury molecule-1
MDA Malondialdehyde
MeSH Medical subject heading
Mfn2 Mitofusin 2
NAG N-acetil-β-D-glicosaminidase
NGAL Neutrophil gelatinase-associated lipocalin
Nox2 NADPH oxidase isoform 2
Nox4 NADPH oxidase isoform 4
Opa1 Optic atrophy 1
PARP Poly-ADP-ribose polymerase
Pck1 Phosphoenolpyruvate carboxykinase 1
PCT Proximal convoluted tubule
PDGFB Platelet-derived growth factor subunit-B
RAAS Renin-angiotensin-aldosterone system
RAGE Receptors for advanced glycation end products
ROS Reactive oxygen species
RPTEC Renal proximal tubule epithelial cells
SGLT2 Sodium-glucose co-transporter 2
SNX Subtotal nephrectomy
SOD1 Superoxide dismutase isoenzyme 1
SOD2 Superoxide dismutase isoenzyme 2
sRAGE Soluble receptor for advanced glycation end products
STZ Streptozotocin
TAC Total antioxidant capacity
TCA Tricarboxylic acid
TGFβ Transforming growth factor beta
TIMP2 Tissue inhibitor of metalloproteinases 2
THBS1 Thrombospondin 1
TLR2 Toll-like receptor 2
TLR4 Toll-like receptor 4
TNC Tenascin C
TNFα Tumor necrosis factor alfa
TOS Total oxidant status
T1DM Type 1 diabetes mellitus
T2DM Type 2 diabetes mellitus
UNX Unilateral nephrectomy
UUO Unilateral ureteric obstruction
WD Western diet
αSMA Alfa-smooth muscle actin
3NT 3-nitrotyrosine
8OHdG 8-hydroxydeoxyguanosin

1. Introduction

Diabetes ranks among the top 10 causes of death worldwide and in the last few years an estimate of 400 to 450 million adults were considered to be affected by this disease, with an expected rising tendency in the incoming years. T2DM plays a chief roll in this scenario, representing between 87% and 95% of the total number of diabetes cases.(1–3)

T2DM is a complex multifactorial metabolic disease, mainly characterized by elevated plasmatic glucose levels. Hyperglycemia in T2DM is thought to arise as a consequence of various factors, such as increased insulin resistance, decreased insulin secretion, increased hepatic glucose production, increased lipolysis, decreased incretin effect, neurotransmitter dysfunction, increased glucagon secretion and increased glucose reabsorption.(1,2,4) Other factors like renin-angiotensin-aldosterone system (RAAS) regulation and vitamin D levels have also been associated with T2DM pathogenesis, further deepening the recognized complexity of this metabolic disease.(5,6) Indeed, the interaction between these factors contributes to a cycle of progressive metabolic deterioration, further increasing hyperglycemia and ultimately affecting various systems and contributing to various complications and the onset of metabolic syndrome, a cluster of risk factors consisting of hypertension, dyslipidemia, hyperglycemia and abdominal obesity.(7,8)

Microvascular and macrovascular complications are common in patients with T2DM. In fact, at the time of clinical diagnosis microvascular complications like retinopathy, peripheral neuropathy and microalbuminuria are already present.(9,10) Moreover, screening for people at high risk of T2DM detected a statistically comparable prevalence of microvascular complications in people with undiagnosed diabetes and people diagnosed in clinical practice, supporting the early onset of these complications in the disease's progression.(10) Although relatively mild in the early stages of T2DM, if left unmanaged, microvascular complications like retinopathy, neuropathy and nephropathy will progressively worsen due to tissue activated inflammatory and fibrotic processes, and lead to more severe morbidity such as blindness, neural dysfunctions and end-stage renal disease, respectively.(11,12) On the other hand, macrovascular complications consist of damage provoked on arteries and smooth muscle, that will lead to increasingly higher risk and incidence of atherosclerosis, coronary artery disease, peripheral arterial disease, stroke and other macrovascular diseases, with consequential higher mortality risk.(11,12)

In the long course of T2DM evolution, rigorous plasmatic glucose control is paramount in the management of T2DM progression and subsequent complications. Besides lifestyle changes

(adopting a balanced diet, weight management, amongst others), an array of pharmacological tools is available and should be used considering each patient's profile and comorbidities.(13,14)

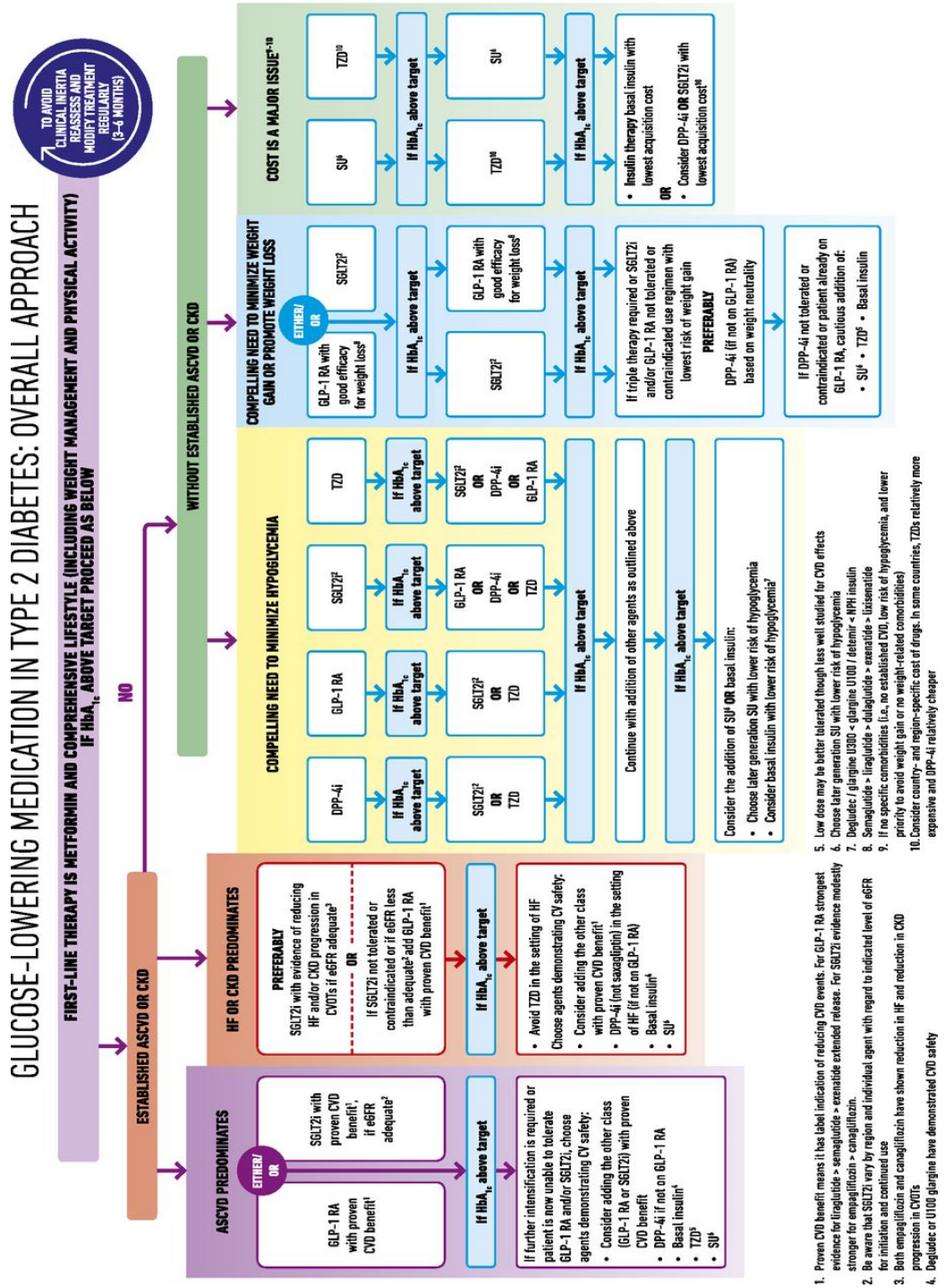

Figure 1 - American Diabetes Association and European Association for the Study of Diabetes consensus algorithm with general recommendations on pharmacotherapeutic approaches for T2DM (Taken from Davies MJ, et al. 2018).(14)

ASCVD: Atherosclerotic cardiovascular disease; CKD: Chronic kidney disease; CVD: Cardiovascular disease; DPP4-i: dipeptidyl peptidase 4 inhibitors; GLP-1 RA: Glucagon-like peptide-1 receptor agonists; HbA1c: Glycosylated hemoglobin A1c SGLT2i: Sodium-glucose co-transporter 2 inhibitors; SU: Sulfonylureas; TZD: thiazolidinediones.

Available options consist primarily of biguanides, iSGLT2, glucagon-like peptide-1 receptor agonists, dipeptidyl peptidase-4 inhibitors, thiazolidinediones, sulfonylureas, insulin and insulin analogs, among other drug classes currently less prevalent in clinical practice. Therapy choice is generally based on recommended algorithms, that can follow an overall approach (Figure 1) in patients with minimal complications or follow specific approaches in patients with more severe complications (for example atherosclerotic cardiovascular disease, chronic kidney disease or the need for weight loss).(14,15)

These algorithms have been updated in the last few years in face of the newer evidence from preclinical and clinical trials, in which iSGLT2 related studies emerge as one of the most heavily researched.(14) iSGLT2 (*e.g.* canagliflozin, dapagliflozin, empagliflozin) are the most recently approved oral drug class for T2DM management that act by increasing glucose urinary excretion. Through selective inhibition of SGLT2-mediated glucose reabsorption in the kidney, iSGTL2 drugs prompt lower plasmatic glucose levels. Sodium-glucose co-transporters are a family of 12 proteins present in epithelial cells that are able of actively transporting glucose in various tissues. Particularly, SGLT2 are ideal targets for modulation of renal glucose excretion as they are almost solely present in the S1 and S2 segments of the proximal convoluted tubule (PCT) and are cumulatively responsible for 90% of the renal glucose reabsorption. With an average of 180 g of filtered glucose per day in healthy subjects, from which about 99% is reabsorbed to blood stream, the kidney-directed mechanism of action of iSGLT2 substances is a valuable therapeutic weapon in almost all subgroups of T2DM patients, being exceptions patients that manifest relevant hypoglycemia or sustained changes in glomerular filtration rate (GFR). Long term glycemic control, commonly measured through glycosylated hemoglobin A1c (HbA1c), is essential in T2DM management and SGLT2 inhibitors are now recognized for their impact on weight loss, reduction of plasma glucose without inducing increased insulin secretion or hypoglycemia, reduction of blood pressure, cardiovascular protection, reduction of hyperuricemia and nephroprotection.(16–18)

Interestingly, the kidney is the main target of iSGLT2 mechanism of action. The kidneys (Figure 2) are two organs that mediate interactions between circulatory and urinary systems and through those interactions, they are capable of regulating hydric, electrolytic and acid-base balances of the body.(19,20) Blood flows to the kidney and into the afferent arterioles, where it derives to glomerular capillaries, which in turn converge to efferent arterioles. It's in glomerular capillaries that we begin to identify the main functional units of the kidney: the nephrons (Figure 3).(19,21)

Nephrons are present in normal kidneys in amounts surrounding 1.0 to 1.2 million nephrons per kidney and are located in the cortex or the cortico-medullary junction. The main structures of the nephron are the afferent and efferent capillaries (glomerular tuft), Bowman's capsule, PCT, loop of Henle, distal convoluted tubule, and the collecting duct. It is along these structures that occur main processes of the nephron: filtration, reabsorption and secretion.(19,22)

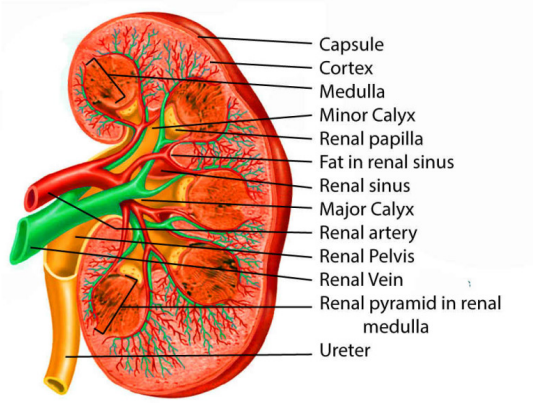

Figure 2 - Kidney general structure and main components (Taken from *Leslie SW, et al. 2019*).(20)

In healthy subjects, filtration occurs passively in the glomerulus where fluid and solutes are pressured into the tubule, with plasmatic components such as water, sodium chloride, glucose, amino acids, creatinine or urea being filtered, and components like proteins and cells following unfiltered to the efferent arterioles. Reabsorption of the filtered components and secretion of plasmatic components may occur through passive diffusion or active transport between the various segments of the tubule and the peritubular capillaries originated from the efferent arterioles. In the PCT occurs the majority of reabsorption, where essentially all filtered glucose and amino acids are reabsorbed, as well as the majority of water and sodium chloride. Furthermore, along the PCT, loop of Henle and distal convoluted tubule occur several reabsorption and secretion processes, mediated by distinct means such as gradients, transporting proteins and hormone interactions, mainly promoting reabsorption of useful substances and secretion of metabolic waste, finally culminating in the excretion of less than 1% of the filtered load into the collecting duct and later into urine. It is through the sum of these processes that the kidney is able to contribute to an overall stable environment for tissue and cell metabolism.(18,19,22)

However, a multitude of factors can influence the normal function and structure of the kidney, contributing to acute damage or disease onset. AKI is characterized by a quick decline in GFR within a period of some hours to a few months, causing retention of metabolic wastes. It can be

caused by factors like ischemia, exogenous toxicity, endogenous toxicity or infection, and can produce vascular, glomerular, tubular and/or interstitial damage.(23)

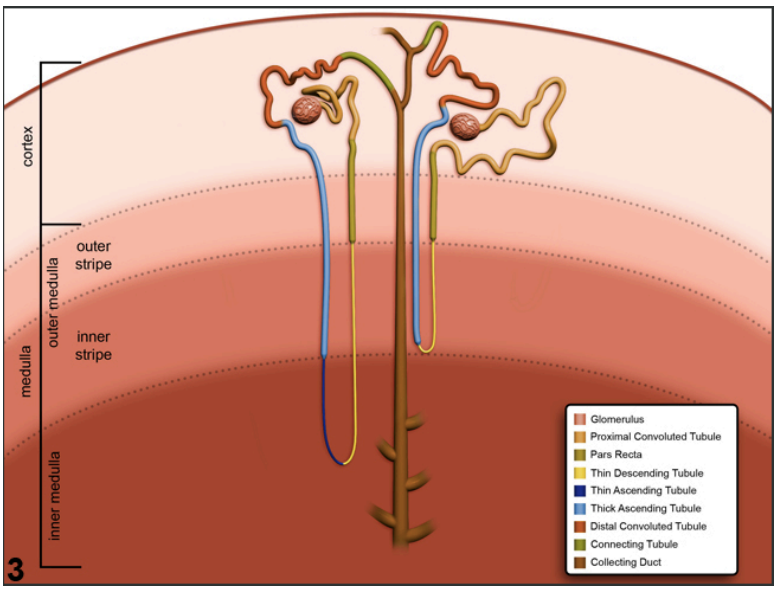

Figure 3 – Detailed constituents of the cortical and cortico-medullar nephrons (Taken from "*Rodriguez F, et al. 2004*").(21)

CKD, on the other hand, is characterized by decreased kidney function, shown by GFR inferior to 60 mL/min/1,73 m^2, and/or at least 1 marker of kidney damage, both measured in a period over 3 months. It can be sub-divided into stages, from G1 (normal function) to G5 (kidney failure or end-stage renal disease), and its causes are heterogenic, contributing to sustained renal injury and development of glomerulosclerosis, tubular atrophy, and interstitial fibrosis. Predominant causes of CKD worldwide are T2DM, hypertension and primary glomerulonephritis.(24)

Diabetic nephropathy is a complex and multifactorial condition, with distinct underlying pathophysiological mechanisms, and is typically characterized in early stages by either microalbuminuria and/or hyperfiltration (i.e. increased GFR).(25–27) Similarly, disease progression can also occur due to various factors. It is understood that metabolic and hemodynamic imbalances, and their interactions, are the main contributors to both disease onset and disease progression. Hyperglycemia, the main player in metabolic renal damage, acts via extracellular and intracellular generation of advanced glycation end-products (AGEs), activation of protein kinase C, and activation of the polyol pathway, all of which contributing to reactive oxygen species (ROS) overproduction.(25,27) Hemodynamic alterations such as hypertension, exerts a physical pressure over renal vascularization and glomerular capillaries, RAAS activation, mainly due to Angiotensin II mediated overproduction of ROS, further contributes to the progression of this disease.(25,27,28) Aforementioned metabolic and hemodynamic alterations

create an environment of oxidative stress that will intensify noxious cell signaling and cytokine production. These mediators contribute to hyperfiltration, exacerbation of angiogenesis, extracellular matrix protein accumulation, inflammatory response and apoptosis, that will ultimately affect the functional and structural composition of the vascular, glomerular, tubular and interstitial ambiance.(27,28) Damage provoked to epithelial and glomerular cells is generally accepted as the most common precursor of diabetic nephropathy, but recent evidence also point towards tubulointerstitial originated nephropathy phenotypes, highlighting the heterogenicity of both diabetic kidney disease inception, progression and eventual kidney failure.(25,27–29)

T2DM patients are at a higher risk of developing renal diseases, namely AKI, CKD, diabetic nephropathy or even an association of the last two.(30) Due to obvious constraints within human experimentation, a proper understand of cellular and molecular mechanisms underlying iSGLT2 nephroprotection has been achieved through *in vitro* and *in vivo* models within preclinical research.

AKI models of injury mimic the rapid and transitory decrease in function through methods such as reduction of renal blood flow (*e.g.* ischemia-reperfusion – [IR] – by surgically clamping the pre-renal arterial), insults to the structural components of the kidney (*e.g.* nephrotoxicity via compounds like gentamicin) or urinary tract obstruction (*e.g.* unilateral ureteric obstruction – [UUO] – or nephrolithiasis via crystal inducing substances like oxalate).(30,31)

Models of CKD focus on whole kidney damage or on segmental damage in specific structures, like the glomerulus or tubules. These models include: i) hypertensive models, the most representative among CKD models, include genetic (*e.g.* Dahl salt-sensitive rat), surgical (*e.g.* subtotal nephrectomy – [SNX] – or unilateral nephrectomy – [UNX]) and toxicity models (*e.g.* administration of adriamycin); ii) auto-imune disease models (*e.g.* IgA nephropathy in ddy mice); iii) models of hereditary diseases (*e.g.* Alport syndrome in alport mice).(30,31)

Diabetic nephropathy animal models may arise from artificial induction, selective breeding and genetical engineering.(32) Artificial induction models consist primarily of pancreatic toxicity induced in rodents through streptozotocin (STZ) administration, which provokes insulin deficiency and induces type 1 diabetes mellitus (T1DM),(33) and dietary imbalances with high-carbohydrate or high-lipid intake (*e.g.* Western diet – [WD]), which contribute to obesity, insulin resistance and consequently T2DM.(32) Various spontaneous diabetic strains of mice and rat are available, where genetic profiles with predisposition for the onset of diabetes are the common denominator. Some of the most notable are Akita mice (deficiency in Insulin-2 folding, leading to

insulin deficiency and stemming T1DM),(34) *db/db* mice (deficiency in leptin receptor, leading to overeating, obesity, insulin resistance, and precipitating T2DM features),(35) BTBR *ob/ob* mice (insulin resistant BTBR mice with deficiency in leptin ligand, leading to obesity associated with insulin resistance, obesity and originating T2DM features),(36) KK-Ay mouse (KK/Ta mouse, a model with mild T2DM phenotypic characteristics, transfected with the Ay obese gene, consequently exhibiting more severe characteristics of T2DM such as obesity, hyperglycemia, high levels of HbA1c and albuminuria),(37) and the OLETF rat (polygenic and sex-dependent model o T2DM, with phenotypical hyperglycemia, polyuria, mild obesity, hypertension, dyslipidemia and diabetic nephropathy).(38) Overlapping different experimental models can also be a tool to replicate the clinical incidence of simultaneous kidney afflictions, as CKD and diabetic nephropathy are commonly found together.(30,31)

At a cellular level, *in vitro* models can also be useful to evaluate signaling pathways and related cellular processes. Although lacking the functional and structural complexity that arise from *in vivo* models, *in vitro* studies allow the identification and comprehension of biomarkers underlying mechanisms involved in nephropathy. Generally, they rely on the cellular exposure to mediators present in pathological conditions such as high glucose, AGEs, transforming growth factor beta (TGFβ), albumin or other proteins. Cell lines can be of human or animal origin and human renal proximal tubule epithelial cells (RPTEC), immortalized human kidney 2 proximal tubule cells (HK2) and spontaneously immortalized pig Lilly Laboratories Cell-Porcine Kidney 1 proximal tubule cells are among the most widely used.(39)

Through quantification of biomarkers and other parameters, it is possible to assess the state and progression of kidney disfunction and injury *in vivo*. Measuring systemic, hemodynamic and cardiorenal parameters like bodyweight, blood pressure or plasmatic glucose, that directly or indirectly influence kidney disease, is important to establish a feasible baseline for interpretation of renal-specific parameters.(40) Kidney damage implies pathologic abnormalities affecting the functional and structural basis of the kidney and can be assessed by biopsy, analytical or imaging methods. In clinical and research settings, kidney function is majorly assessed by GFR that can be estimated with endogenous or exogenous markers such as plasmatic creatinine, plasmatic cystatin C, plasmatic blood urea nitrogen (BUN) or urinary inulin.(41) Loss of kidney function can be indicated by deviations from standard values in these parameters, or by appearance of renal damage indicators like albuminuria, proteinuria or polyuria.(41) As renal damage chronically evolves, biomarkers like nephrin (an indicator of glomerular injury), kidney injury molecule-1 (KIM1) (an indicator of tubular damage), neutrophil gelatinase-associated lipocalin (NGAL) (an

indicator of tubulointerstitial injury), N-acetil-β-D-glicosaminidase (NAG) (and indicator of proximal tubule damage), and alfa-smooth muscle actin (αSMA) or collagen (indicators of fibrotic processes) are useful.(41–43)

Moreover, kidney histology is a valid resource in experimental settings to analyze morphology. Such methods may help to perceive structural injury and precise the location of damage. Useful approaches include distinct stainings such as hematoxylin and eosin (enabling analysis of general cellular integrity), periodic acid Schiff's (enabling visualization of glomerular and tubular membranes), Masson's trichrome or Sirius Red (enabling visualization of fibrosis), or immunostaining with monoclonal antibody ED1 (enabling visualization of macrophage infiltration and assessment of inflammation), among many others.(44–46)

Finally, it is relevant to assess cellular parameters and molecular pathways that underlies kidney injury. Detecting markers of oxidative stress (*e.g.* malondialdehyde – [MDA] - and 8-hydroxydeoxyguanosine – [8OHdG]), inflammatory processes (*e.g.* TGFβ and macrophage chemoattractant protein-1) and apoptosis (*e.g.* mitofusin 2 – [Mfn2] - and optic atrophy 1 – [Opa1]) are important to understand renal disease progression in general, along with glucose metabolism pathways-related markers, important in diabetic nephropathy in particular.(47–50)

Based on the growing clinical evidence of nephroprotection provided by the antidiabetic iSGLT2 drugs,(51,52) the mains goals of present work are twofold: 1) to provide an updated review focused on physiological/cellular mechanisms underlying iSGLT2 nephroprotection. Moreover, a proper clarification of such mechanisms also allows 2) the identification of putative side effects iSGLT2- driven.

2. Methods

Data collection was based on primary research works published between January 2013 and December 2018 in English language. Studies containing pre-clinical evidence from *in vitro* models and *in vivo* models of kidney disease treated with iSGLT2 substances were obtained by Pubmed search. The search was conducted using Medical subject heading (MeSH) terms and keywords related to SGLT2 inhibitors and renoprotection (Figure 4) combined with boolean operators AND/OR. A total of 80 records were obtained from the search. Searching in different databases did not yield relevant results over the 80 records obtained in PubMed search.

PubMed: (((((((((SGLT2 inhibitors) OR iSGLT2) OR canagliflozin) OR dapagliflozin) OR empagliflozin) OR ertugliflozin) OR ipragliflozin) OR luseogliflozin) OR tofogliflozin) AND (((((renoprotection) OR renoprotective) OR kidney injury) OR kidney disease) OR renal damage) AND (((((In vitro) OR In vivo) OR rodents) OR mice) OR rats)

Figure 4 - MeSH terms and keywords used in Pubmed literature review.

Abstracts of selected articles were screened for relevance. The inclusion of studies in this review was based in works focused on mechanisms or biomarkers related to renal benefits of SGLT2 inhibitors (total excluded: 41 records). Full texts of the selected abstracts were reviewed for eligibility (total excluded: 6 records). Screening for additional data in the selected articles did not yield further relevant studies. The final number of reports included in the present review is 33 records (Figure 5).

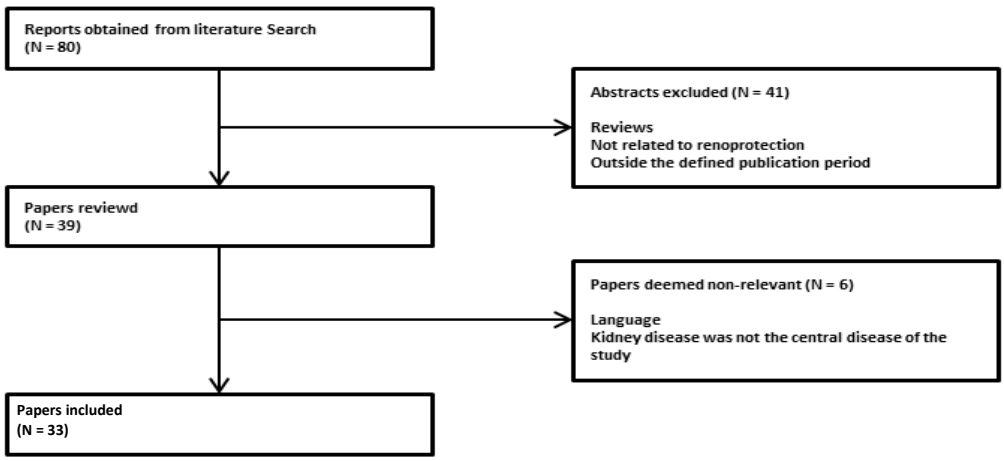

Figure 5 - Flow diagram illustrating the search strategy.

In each paper, quantitative parameters were compiled and assessed for relevance. When repeated measures of a certain feature were conducted, only the final observation recorded was considered in present work. Key findings of iSGLT2 effects on renal damage were obtained from the comparisons and statistical analysis provided by authors between kidney disease experimental models treated with iSGTL2 compounds versus those without treatment. A total of 791 parameters were compiled.

Parameters measured in organs other than the kidney (total: 40) and measured in humans (total: 14) were excluded. Parameters considered not relevant for the present study, such as water intake or survival, were excluded (total: 45). Parameters without statistical significance were excluded (total: 146). A total of 546 parameters were included in the final review.

In order to enhance the readability of this work, results are structured in 3 distinct sections: 3.1 (influence of iSGLT2 on systemic features), 3.2 (influence of iSGLT2 on kidney morphology and function) and 3.3 (influence of iSGLT2 on cellular and molecular mechanisms underlying renal injury).

3. Results

Herein, we describe the main results from the 33 studies included in this review. Some of the studies conducted multiple experiments relevant to our goal, corresponding to a total of 9 *in vitro* (53–60) and 33 *in vivo* (55,57–85) experiments.

Table 1 - Main aspects of selected experimental models

Category	iSGLT2	Dosage	Experimental model	Experiment duration	Reference
DN	dapagliflozin	0,1-1,0 mg/kg/day	*db/db* mice	12 weeks	(60)
		1 mg/kg/day	*db/db* mice	12 weeks	(64)
			Fructose fed STZ-Wistar rats	8 weeks	(71)
			HFD fed Wistar rats	20 weeks	(63)
			OLEFT rats	12 weeks	(73)
		2 mg/kg/day	STZ-Wistar rats	12 weeks	(82)
		5 mg/kg/day	WD fed C57BL/6 mice	26 weeks	(79)
	empagliflozin	10 mg/kg/day	*db/db* mice	10 weeks	(84)
				5 weeks	(59)
			STZ-eNOS knockout C57BL/6 mice	19 weeks	(85)
			STZ-Sprague Dawley rats	4 weeks	(70)
		30 mg/kg/day	BTBR *ob/ob* mice	12 weeks	(61)
			BTBR *ob/ob* mice + hypertension	6 weeks	(61)
		70 mg/kg/day	Ins2+/Akita mice	15 weeks	(78)
	ipragliflozin	0,3-3,0 mg/kg/day	*db/db* mice	8 weeks	(65)
			STZ-BALB/c mice	2 weeks	(65)
		10 mg/kg/day	HFD fed C57BL/6 mice	16 weeks	(57)
		4 mg/kg/day	BTBR *ob/ob* mice	18 weeks	(76)
	luseogliflozin	10 mg/kg/day	STZ-Dahl rats	8 weeks	(66)
		10 mg/kg/day	T2DN rats	12 weeks	(67)
	tofogliflozin	5,0-15,0 mg/kg/day	*db/db* mice	8 weeks	(69)
			KK-Ay/Ta mice	5 weeks	(62)
DN + CKD	dapagliflozin	1 mg/kg/day	UNX *db/db* mice	14 weeks	(77)
	ipragliflozin	0,1-3,0 mg/kg/day	UNX STZ-ICR mice	7 weeks	(75)
CKD	dapagliflozin	1 mg/kg/day	SNX Sprague Dawley rats	12 weeks	(80)
				8 weeks	(72)
		1,5 mg/kg/day	UNX Protein-overload proteinuria C57BL/6 mice	23 days	(83)
	ipragliflozin	0,1-3,0 mg/kg/day	UNX KK-Ay mice	4 weeks	(74)
	luseogliflozin	30 mg/kg/day	IR-C57BL/6 mice	4 weeks	(58)
AKI	dapagliflozin	10 mg/kg/day	IR-C57BL/6 mice	48 hours	(55)
	empagliflozin	10 mg/kg/day	High-oxalate fed C57BL/6 mice	2 weeks	(68)
			UUO Wistar rats	3 weeks	(81)
	luseogliflozin	30 mg/kg/day	UNX IR-C57BL/6 mice	1 week	(58)
in vitro	canagliflozin	500 nM	HK-2 cells + TGFβ	24 hours	(53)
	dapagliflozin	0,2-20,0 µM	mProx24 cells + HG	24 hours	(60)
		1-10 µM	HK-2 cells + Hypoxia	30 minutes	(55)
		10-100 µM	HK-2 cells + HG	48 hours	(56)
	empagliflozin	100-500 nM	HK-2 cells + HG	72 hours	(54)
		500 nM	HK-2 cells + HG	6 hours	(59)
			RPTEC cells + TGFβ	24 hours	(53)
	ipragliflozin	10 nmol/L	HK-2 cells + Palmitate	48 hours	(57)
	luseogliflozin	100 nmol/L	mProx24 cells + Hypoxia	26 hours	(58)

AKI: Acute kidney injury; CKD: Chronic kidney disease; DN: Diabetic nephropathy; HFD: High-fat diet; HG: High glucose; HK2: Human kidney 2 proximal tubule; RPTEC: Renal proximal tubule epithelial cells; SNX: Subtotal nephrectomy; STZ: Streptozotocin; UNX: Unilateral nephrectomy; UUO: Unilateral ureteric obstruction; WD: Western diet;

Distinct methodological approaches were used to replicate experimental features of renal damage. High glucose and hypoxia conditions were the main methodological approaches to elicit renal insult during *in vitro* experiments. Considering *in vivo* models of renal injury, both diabetic

(genetic-, chemical- and/or diet-induced) and non-diabetic (nephrectomy, ureteric obstruction, IR) rodent models were selected from an array of animal strains (C57BL/6 mice, Wistar rats, Sprague-Dawley rats, Dahl rats, BALD/c mice, T2DN rats, BTBR mice, KK-Ay mice, ICR mice and Akita mice). Animal experiments comprised models of AKI, CKD and diabetic nephropathy. SGLT2 inhibitors comprised the active substances canagliflozin (only used on *in vivo* experimental models) as well as dapagliflozin, empagliflozin, ipragliflozin, luseogliflozin and tofogliflozin (only used on *in vivo* experimental models). A synthesis of these data is shown in Table 1.

3.1. Influence of iSGLT2 on systemic features

We started with the analysis of *in vivo* evidence focused on the influence of SGLT2 inhibitors on systemic pathophysiological features, particularly those that characterize T2DM.

3.1.1. Body and fat weight

Opposing evidence was observed regarding SGLT2 inhibitors impact on body weight. While SGLT2 inhibitors have shown a relevant effect in reducing body weight in 6 studies, the remaining ones detected a relevant increase in this parameter. Particularly, dapagliflozin and luseogliflozin contributed to both outcomes in different experimental models. Visceral fat weight versus body weight ratio was significantly reduced upon dapagliflozin (1 mg/kg/day) treatment (Table 2).

Table 2 - Effect of iSGLT2 on body and fat weight

Parameter	Effect	iSGLT2	Dosage	Experimental model	Reference
Body weight	(-)	dapagliflozin	1 mg/kg/day	HFD fed Wistar rats	(63)
			5 mg/kg/day	WD fed C57BL/6 mice	(79)
		ipragliflozin	0,1-3,0 mg/kg/day	UNX STZ-ICR mice	(75)
			1,0-3,0 mg/kg/day	UNX KK-Ay mice	(74)
			3,0 mg/kg/day	*db/db* mice	(65)
		luseogliflozin	10 mg/kg/day	T2DN rats	(67)
	(+)	dapagliflozin	0,1-1,0 mg/kg/day	*db/db* mice	(60)
		empagliflozin	10 mg/kg/day	*db/db* mice	(84)
			70 mg/kg/day	Ins2+/Akita mice	(78)
		luseogliflozin	10 mg/kg/day	STZ-Dahl rats	(66)
		tofogliflozin	5,0-15,0 mg/kg/day	*db/db* mice	(69)
	(=)	dapagliflozin	1 mg/kg/day	*db/db* mice	(64)
				OLEFT rats	(73)
				UNX *db/db* mice	(77)
		empagliflozin	10 mg/kg/day	STZ-eNOS knockout C57BL/6 mice	(85)
				STZ-Sprague Dawley rats	(70)
			30 mg/kg/day	BTBR *ob/ob* mice	(61)
		ipragliflozin	10 mg/kg/day	HFD fed C57BL/6 mice	(57)
			4 mg/kg/day	BTBR *ob/ob* mice	(76)
		tofogliflozin	5,0-15,0 mg/kg/day	KK-Ay/Ta mice	(62)
Visceral fat weight/Body weight ratio	(-)	dapagliflozin	1 mg/kg/day	HFD fed Wistar rats	(63)

The effect column sums up the information available in all included studies. (-) statistically significant decrease; (+) statistically significant increase; (=) absence of statistically significant differences. HFD: High fat diet; SNX: Subtotal nephrectomy; STZ: Streptozotocin; UNX: Unilateral nephrectomy; WD: Western diet;

3.1.2. Metabolic profile

A significant reduction of plasmatic glucose levels was observed upon iSGLT2 treatment in the large majority of studies included in this review, with 3 experiments failing to achieve the same reduction. Consequently, it would be expected a similar pattern of HbA1c levels, which was the case in every study assessed. Insulin concentration in the blood was lowered upon iSGLT2 action in all studies, with the exception of an experimental model of STZ induced diabetes. Both glucose and insulin tolerance were ameliorated in almost all treated subgroups, with both parameters failing to have a statistically significant improvement in a single study of a *db/db* mice model. In this case, dapagliflozin failed to improve glucose and insulin tolerance and also aggravated pyruvate tolerance by the end of the 24 weeks experiment (Table 3).

Interestingly, plasmatic leptin and fibroblast growth factor 21 (FGF21) levels had a significant decrease by iSGLT2 action. Finally, metabolic improvement was also observed within lipidic field with both plasmatic cholesterol and triglycerides showing a statistically decreased levels in iSGLT2 treated groups (Table 3).

Table 3 - Effect of iSGLT2 on metabolic profile of renal-damage models

Parameter	Effect	iSGLT2	Dosage	Experimental model	Reference
Plasma glucose	(-)	dapagliflozin	1 mg/kg/day	*db/db* mice	(64)
				db/db mice	(60)
				OLEFT rats	(73)
				UNX *db/db* mice	(77)
			1,5 mg/kg/day	UNX Protein-overload proteinuria C57BL/6 mice	(83)
			2 mg/kg/day	STZ-Wistar rats	(82)
			5 mg/kg/day	WD fed C57BL/6 mice	(79)
		empagliflozin	10 mg/kg/day	*db/db* mice	(84)
				STZ-Sprague Dawley rats	(70)
			70 mg/kg/day	Ins2+/Akita mice	(78)
			30 mg/kg/day	BTBR *ob/ob* mice	(61)
		ipragliflozin	0,3-3,0 mg/kg/day	UNX KK-Ay mice	(74)
			1,0-3,0 mg/kg/day	UNX STZ-ICR mice	(75)
			3,0 mg/kg/day	*db/db* mice	(65)
				STZ-BALB/c mice	(65)
			4 mg/kg/day	BTBR *ob/ob* mice	(76)
		luseogliflozin	10 mg/kg/day	STZ-Dahl rats	(66)
				T2DN rats	(67)
		tofogliflozin	5,0-15,0 mg/kg/day	KK-Ay/Ta mice	(62)
				db/db mice	(69)
	(=)	empagliflozin	10 mg/kg/day	STZ-eNOS knockout C57BL/6 mice	(85)
				High oxalate fed C57BL/6 mice	(68)
HbA1c	(-)	dapagliflozin	1 mg/kg/day	OLEFT rats	(73)
				UNX *db/db* mice	(77)
				db/db mice	(60)
		empagliflozin	10 mg/kg/day	*db/db* mice	(84)
				STZ-Sprague Dawley rats	(70)
		ipragliflozin	0,3-3,0 mg/kg/day	UNX KK-Ay mice	(74)
			1,0-3,0 mg/kg/day	UNX STZ-ICR mice	(75)
		luseogliflozin	10 mg/kg/day	STZ-Dahl rats	(66)
				T2DN rats	(67)
		tofogliflozin	5,0-15,0 mg/kg/day	*db/db* mice	(69)
Plasma insulin	(-)	dapagliflozin	1 mg/kg/day	HFD fed Wistar rats	(63)
			5 mg/kg/day	WD fed C57BL/6 mice	(79)

Parameter	Effect	iSGLT2	Dosage	Experimental model	Reference
		empagliflozin	70 mg/kg/day	Ins2+/Akita mice	(78)
		ipragliflozin	1,0-3,0 mg/kg/day	UNX KK-Ay mice	(74)
				UNX STZ-ICR mice	(75)
		luseogliflozin	10 mg/kg/day	T2DN rats	(67)
	(=)	luseogliflozin	10 mg/kg/day	STZ-Dahl rats	(66)
Glucose tolerance	(+)	dapagliflozin	1 mg/kg/day	HFD fed Wistar rats	(63)
				OLEFT rats	(73)
		ipragliflozin	1,0-3,0 mg/kg/day	UNX KK-Ay mice	(74)
				UNX STZ-ICR mice	(75)
	(=)	dapagliflozin	1 mg/kg/day	*db/db* mice	(64)
Pyruvate tolerance	(-)	dapagliflozin	1 mg/kg/day	*db/db* mice	(64)
Insulin tolerance	(+)	ipragliflozin	1,0-3,0 mg/kg/day	UNX KK-Ay mice	(74)
				UNX STZ-ICR mice	(75)
	(=)	dapagliflozin	1 mg/kg/day	*db/db* mice	(64)
Insulin resistance	(-)	dapagliflozin	1 mg/kg/day	HFD fed Wistar rats	(63)
		ipragliflozin	1,0-3,0 mg/kg/day	UNX KK-Ay mice	(74)
				UNX STZ-ICR mice	(75)
Plasma cholesterol	(-)	dapagliflozin	1 mg/kg/day	HFD fed Wistar rats	(63)
			5 mg/kg/day	WD fed C57BL/6 mice	(79)
		ipragliflozin	1,0-3,0 mg/kg/day	UNX KK-Ay mice	(74)
Plasma triglycerides	(-)	dapagliflozin	5 mg/kg/day	WD fed C57BL/6 mice	(79)
		ipragliflozin	1,0-3,0 mg/kg/day	UNX KK-Ay mice	(74)
				UNX STZ-ICR mice	(75)
Plasma leptin	(-)	ipragliflozin	1,0-3,0 mg/kg/day	UNX KK-Ay mice	(74)
			3,0 mg/kg/day	UNX STZ- ICR mice	(75)
Plasma FGF21	(-)	ipragliflozin	1,0-3,0 mg/kg/day	UNX KK-Ay mice	(74)
			3,0 mg/kg/day	UNX STZ-ICR mice	(75)

The effect column sums up the information available in all included studies. (-) indicates a statistically significant decrease in the parameter; (+) indicates a significant increase in the parameter; (=) indicates there was no significant differences in the parameter; FGF21: Fibroblast growth factor 21; HbA1c: Glycosylated hemoglobin A1c; HFD: High-fat diet; SNX: Subtotal nephrectomy; STZ: Streptozotocin induced diabetes; UNX: Unilateral nephrectomy; WD: Western diet;

3.1.3. Glucose transporters and related signaling pathways

In order to evaluate the impact of iSGLT2 on glucose related imbalances associated with T2DM, some studies explored the ability of iSGLT2 to induce significant changes in key glucose transporters and/or to modulate related metabolic pathways.

Amongst all studied glucose transporters (Table 4), only SGLT2 was shown to significantly alter the basal expression. Cellular glucose content was significantly reduced by iSGLT2 molecules in an *in vitro* model of hypoxic HK2 cells and in an *in vivo* model of IR C57BL/6 mice and remained unchanged in other 2 *in vivo* experiments.

Enzymes phosphoenolpyruvate carboxykinase 1 (Pck1) and glucose-6-phosphatase (G6p) were the only gluconeogenic enzymes studied in the included studies of this review. The expression of both enzymes was significantly enhanced upon iSGLT2 treatment. However, Pck1 had different outcomes in other 2 studies, remaining unchanged in an experimental model of *db/db* mice treated with empagliflozin and being significantly reduced in a second experimental model of Ins2+/Akita mice treated with empagliflozin (Table 4).

Regarding glucose signaling pathways, one group of investigators assessed glucose metabolic pathways in a renal-damage model of BTBR *ob/ob* mice. Researchers observed a significant shift towards the polyol pathway (as evidenced by the elevated fructose content in the diabetic kidney)

and the tricarboxylic acid (TCA) pathway (were the citrate, cis-aconitate and 2-oxo-glutarate metabolites levels displayed the most noticeable increase). Ipraglifozin successfully lowered the concentration of TCA metabolites, whereas fructose content remained unchanged. Finally, the presence of ipragliflozin significantly lowered the total glucose metabolites concentration in BTBR *ob/ob* mice (Table 4).

Table 4 - Effect of iSGLT2 on key glucose transporters and components of glucose metabolic pathways

Parameter	Effect	iSGLT2	Dosage	Experimental model	Reference
SGLT1*	(=)	dapagliflozin	1 mg/kg/day	HFD fed Wistar rats	(63)
		empagliflozin	70 mg/kg/day	Ins2+/Akita mice	(78)
			30 mg/kg/day	BTBR *ob/ob* mice	(61)
SGLT1#	(-)	empagliflozin	10 mg/kg/day	STZ-Sprague Dawley rats	(70)
	(=)	empagliflozin	10 mg/kg/day	*db/db* mice	(84)
			70 mg/kg/day	Ins2+/Akita mice	(78)
			30 mg/kg/day	BTBR *ob/ob* mice	(61)
SGLT2*	(-)	dapagliflozin	1-10 µM	HK2 cells + Hypoxia	(55)
	(=)	empagliflozin	70 mg/kg/day	Ins2+/Akita mice	(78)
SGLT2#	(-)	empagliflozin	70 mg/kg/day	Ins2+/Akita mice	(78)
	(=)	empagliflozin	10 mg/kg/day	*db/db* mice	(84)
GLUT1#	(-)	empagliflozin	70 mg/kg/day	Ins2+/Akita mice	(78)
GLUT2*	(=)	luseogliflozin	30 mg/kg/day	IR-C57BL/6 mice	(58)
GLUT2#	(-)	empagliflozin	70 mg/kg/day	Ins2+/Akita mice	(78)
	(=)	empagliflozin	10 mg/kg/day	*db/db* mice	(84)
G6P	(+)	dapagliflozin	1 mg/kg/day	*db/db* mice	(64)
Pck1	(+)	dapagliflozin	1 mg/kg/day	*db/db* mice	(64)
	(-)	empagliflozin	70 mg/kg/day	Ins2+/Akita mice	(78)
	(=)	empagliflozin	10 mg/kg/day	*db/db* mice	(84)
Cytosolic glucose content	(-)	dapagliflozin	1-10 µM	HK2 cells + Hypoxia	(55)
	(=)	empagliflozin	10 mg/kg/day	*db/db* mice	(84)
		ipragliflozin	4 mg/kg/day	BTBR *ob/ob* mice	(76)
NBDG	(-)	luseogliflozin	30 mg/kg/day	IR-C57BL/6 mice	(58)
Cytosolic fructose content	(=)	ipragliflozin	4 mg/kg/day	BTBR *ob/ob* mice	(76)
TCA metabolites	(-)	ipragliflozin	4 mg/kg/day	BTBR *ob/ob* mice	(76)
Total glucose metabolites	(-)	ipragliflozin	4 mg/kg/day	BTBR *ob/ob* mice	(76)

The effect column sums up the information available in all included studies. # indicates that the parameter was assessed by mRNA expression levels; (-) indicates a statistically significant decrease in the parameter; (+) indicates a significant increase in the parameter; (=) indicates there was no significant differences in the parameter. GLUT1: Glucose transporter 1; GLUT2: Glucose transporter 2; G6p: Glucose-6-phosphatase; HFD: High-fat diet; HK2: Human kidney 2 proximal tubule; IR: Ischemia-reperfusion; NBDG: fluorescent 2-NBD Glucose; Pck1: Phosphoenolpyruvate carboxykinase 1; SGLT1: Sodium-glucose co-transporter 1; SGLT2: Sodium-glucose co-transporter 2; SNX: Subtotal nephrectomy; STZ: Streptozotocin induced diabetes; TCA: Tricarboxylic acid; UNX: Unilateral nephrectomy;

3.1.4. Cardiorenal and hemodynamic features

Several cardiovascular and hemodynamic features, such as heart rate, mean blood pressure, diastolic blood pressure levels remained unchanged in the presence of any iSGLT2 drug. Yet, systolic blood pressure had some evidence pointing towards benefic effects of iSGLT2 substances in lowering those values, with 4 trials reporting a statistically relevant reduction, whereas in 5 trials no significant changes were observed (Table 5).

Similarly, plasmatic aldosterone and urinary aldosterone concentrations did not present significant changes between renal injury models with or without treatment. The only study reporting plasmatic renin levels showed that in a *db/db* mice model, renin concentration was higher in mice treated with empagliflozin relative to mice with no treatment. Various RAAS components were lowered in OLEFT rats treated with dapagliflozin, as described in a study

showing a significant decrease in urinary angiotensinogen, urinary angiotensin II and cortical angiotensin II receptor type 1 (AT1) (Table 5).

Table 5 - Effects of iSGLT2 treatment in cardiorenal and hemodynamic features

Parameter	Effect	iSGLT2	Dosage	Experimental model	Reference
Heart rate	(=)	empagliflozin	10 mg/kg/day	STZ-Sprague Dawley rats	(70)
Mean Blood Pressure	(=)	luseogliflozin	10 mg/kg/day	STZ-Dahl rats	(66)
				T2DN rats	(67)
Systolic Blood Pressure	(-)	dapagliflozin	1 mg/kg/day	SNX Sprague Dawley rats	(72)
		empagliflozin	70 mg/kg/day	Ins2+/Akita mice	(78)
		ipragliflozin	1,0-3,0 mg/kg/day	UNX KK-Ay mice	(74)
				UNX STZ-ICR mice	(75)
	(=)	dapagliflozin	1 mg/kg/day	SNX Sprague Dawley rats	(80)
		empagliflozin	30 mg/kg/day	BTBR *ob/ob* mice	(61)
		ipragliflozin	0,3-3,0 mg/kg/day	*db/db* mice	(65)
		luseogliflozin	10 mg/kg/day	T2DN rats	(67)
		tofogliflozin	5,0-15,0 mg/kg/day	KK-Ay/Ta mice	(62)
Diastolic blood pressure	(=)	luseogliflozin	10 mg/kg/day	T2DN rats	(67)
Plasma renin	(+)	empagliflozin	10 mg/kg/day	*db/db* mice	(84)
Plasma aldosterone	(=)	empagliflozin	70 mg/kg/day	Ins2+/Akita mice	(78)
Urinary angiotensinogen	(-)	dapagliflozin	1 mg/kg/day	OLEFT rats	(73)
Urinary angiotensin II	(-)	dapagliflozin	1 mg/kg/day	OLEFT rats	(73)
Urinary aldosterone	(=)	dapagliflozin	1 mg/kg/day	UNX *db/db* mice	(77)
Cortical AT1	(-)	dapagliflozin	1 mg/kg/day	OLEFT rats	(73)

The effect column sums up the information available in all included studies. (-) indicates a statistically significant decrease in the parameter; (+) indicates a significant increase in the parameter; (=) indicates there was no significant differences in the parameter. AT1: angiotensin II receptor type 1; SNX: Subtotal nephrectomy; STZ: Streptozotocin induced diabetes; UNX: Unilateral nephrectomy;

3.2. Influence of iSGLT2 on kidney morphology and function

We next examined the available evidence regarding iSGLT2 effects on kidney function and morphological features. Histology and morphology data, serum and urinary markers, and tissue markers are hereby presented.

3.2.1 Kidney histology and morphological features

Whole kidney features were evaluated for iSGLT2 impact. A total of 5 studies reported a significant decrease in kidney weight due to treatment with a SGLT2 inhibitor.(66,74,75,78,82) Cortical area was evaluated in one of the studies where ipragliflozin significantly decreased its volume.(65) Whole kidney deposition of calcium oxalate was not changed,(68) but proteins(66) and triglycerides(63,79) were significantly lower in the presence of iSGLT2 substances.

Total kidney fibrosis was thoroughly assessed in studies included in this work. Cortical fibrosis(67) and medullary fibrosis(66) were reduced in one study, whereas 3 different studies reported a significant reduction in kidney fibrotic area upon iSGLT2 treatments (Figure 6).(58,60,73)

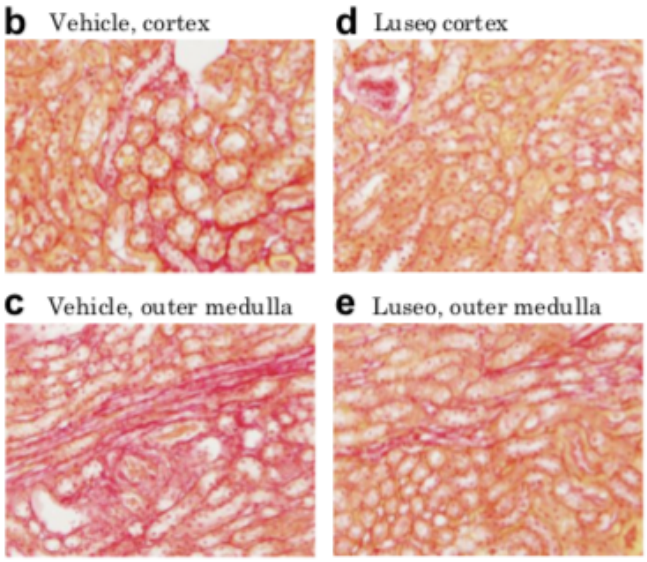

Figure 6 - Representative kidney sections of IR C57BL/6 mice without treatment (b,c) versus IR C57BL/6 mice treated with luseogliflozin. Staining was performed with Sirius-Red (Taken from *Zhang Y, et al. 2018*).(58)

Renal circulation had some improvement due to iSGLT2 action, namely with the reduction of renal vascular pressure(67), renal periarterial fibrosis(59) and endothelial factor CD31(58). SGLT2 inhibitor luseogliflozin also significantly increased vascular endothelial growth factor A in both *in vitro* and *in vivo* (58). Lastly, damage assessed by cortical hypoxia score(65) and congestion/hemorrhage score(58) was significantly reduced in the presence of iSGLT2 drugs.

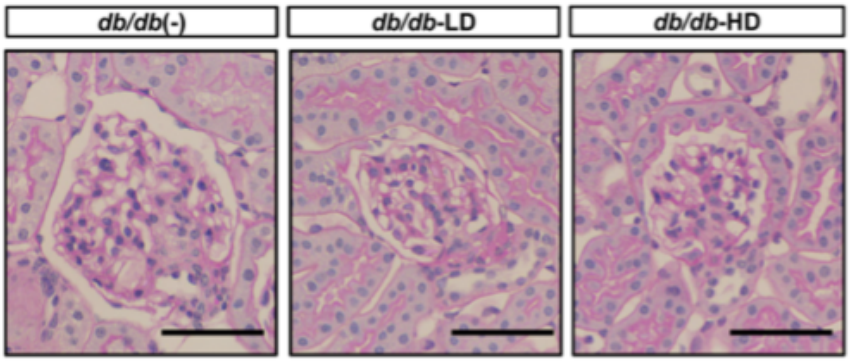

Figure 7 - Representative glomerular size of *db/db* mice without treatment (-) versus *db/db* mice treated with low dose (LD) and high dose (HD) of dapagliflozin. Staining was performed with Periodic acid-Schiff (Taken from *Kamezaki M, et al. 2018*).(65)

Regarding glomerular features, 4 experiments reported a decrease in glomerular size (Figure 7).(61,65,69,78) Podocyte density was increased in the single study that investigated this parameter. Damage coefficients included mesangial matrix score (reduced in 4 different experiments),(60,61,73,79) glomerular injury score (reduced in 4 different experiments),(66,67,82,85) and glomerulosclerosis index (reduced in 3 different experiments).(74,75,77)

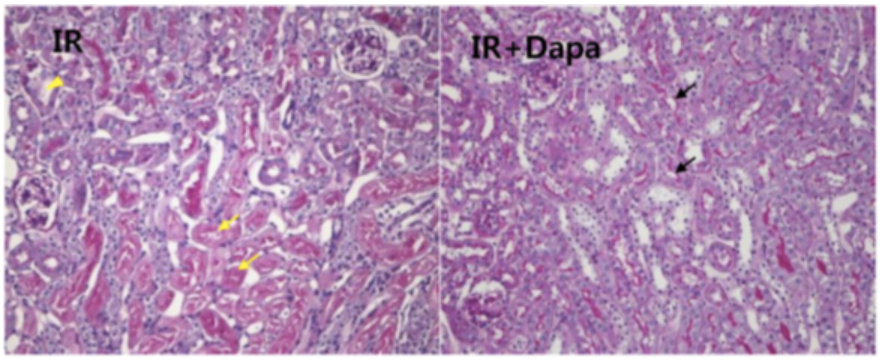

Figure 8 - Representative kidney section of IR C57BL/6 mice without treatment (IR) versus IR C57BL/6 mice treated with dapagliflozin (IR+Dapa). Staining was performed with Periodic acid-Schiff. Original investigators pointed the following remarks: Yellow arrows identify necrotized tubules or cast formation. Yellow arrowheads identify loss of brush border or dilated tubules. Black arrows identify brush border (Taken from *Chang Y-K, et al. 2016*).(55)

Histologic visualization of nephron tubules showed tubular atrophy and empagliflozin was unable to revert this effect.(85) Pinpointed fibrosis, as assessed by tubulointerstitial total collagen, also had no significant changes in the 2 distinct experiments performed in the same study.(84) Qualification of damage yielded a significant decrease in all of the 4 experiments that investigated tubulointerstitial injury score.(55,59,74,75) Interestingly, with iSGLT2 treatment, tubular injury score was reduced in 2 experiments but was increased in another experiment (Figure 8).(55,64,75)

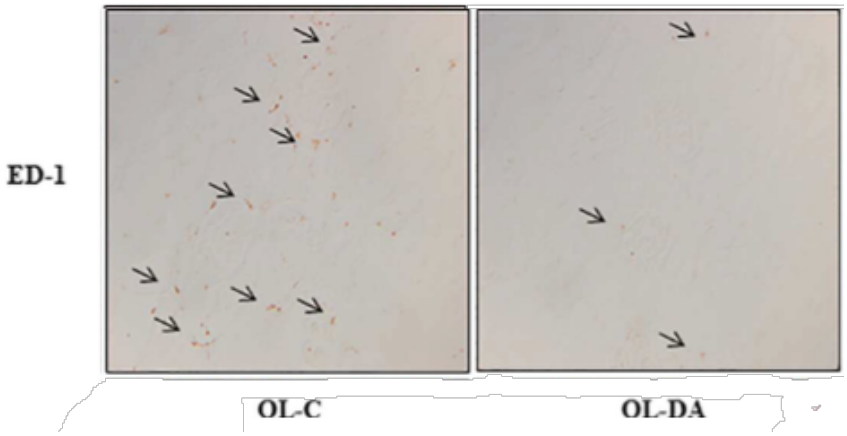

Figure 9 - Immunohistochemistry of macrophage infiltration in OLEFT rats treated with control versus treated with dapagliflozin (Taken from *Shin SJ, et al. 2016*).(73)

Finally, immune response features were also investigated through histology and imaging. Immunohistochemistry targeting cluster of differentiation 68 (CD68) with ED1 antibody revealed that there was a significant decrease in macrophage infiltration in 5 experiments (Figure 9).(60,70,73,83) Basophilic score and inflammatory cell infiltration score were reduced in 2 experiments.(74,75)

3.2.2. Kidney function (Serum and urinary markers)

Numerous serum and urine parameters are commonly evaluated as means to assess renal function. So, a substantial number of those markers were comprised in the studies included for this review.

In the majority of those works, glomerular filtration indicators such as BUN, serum creatinine and GFR showed a significant decrease in their values due to iSGLT2 action. Proteinuria was also lowered in a minority of studies, remaining unaltered in the majority of experiments upon iSGLT2 treatment. Albuminuria and the closely tied albumin-to-creatine ratio were predominantly lower in animals treated with an iSGLT2 drug, but one study conducted in *db/db* mice retrieved opposite results for both parameters. Finally, creatinine clearance and urine volume had the most controversial results, with at least two experimental models reporting one of the three possible effects: parameter lowered when iSGLT2 was given, parameter raised when iSGLT2 was given and parameter unaffected by iSGLT2 action (Table 6).

Table 6 - Effects of iSGLT2 in serum and urinary markers of kidney function

Parameter	Effect	iSGLT2	Dosage	Experimental model	Reference
BUN	(-)	dapagliflozin	10 mg/kg/day	IR-C57BL/6 mice	(55)
			2 mg/kg/day	STZ-Wistar rats	(82)
		empagliflozin	10 mg/kg/day	UUO Wistar rats	(81)
	(=)	empagliflozin	10 mg/kg/day	High oxalate fed C57BL/6 mice	(68)
Serum creatinine	(-)	dapagliflozin	1 mg/kg/day	HFD fed Wistar rats	(63)
			1 mg/kg/day	OLEFT rats	(73)
			10 mg/kg/day	IR-C57BL/6 mice	(55)
			2 mg/kg/day	STZ-Wistar rats	(82)
		empagliflozin	10 mg/kg/day	UUO Wistar rats	(81)
		ipragliflozin	1,0-3,0 mg/kg/day	UNX KK-Ay mice	(74)
		ipragliflozin	3,0 mg/kg/day	UNX STZ-ICR mice	(75)
	(=)	empagliflozin	10 mg/kg/day	High oxalate fed C57BL/6 mice	(68)
				STZ-Sprague Dawley rats	(70)
		luseogliflozin	30 mg/kg/day	IR-C57BL/6 mice	(58)
GFR	(-)	dapagliflozin	1 mg/kg/day	SNX Sprague Dawley rats	(80)
		empagliflozin	70 mg/kg/day	Ins2+/Akita mice	(78)
		luseogliflozin	10 mg/kg/day	STZ-Dahl rats	(66)
				T2DN rats	(67)
	(=)	dapagliflozin	1 mg/kg/day	SNX Sprague Dawley rats	(72)
		empagliflozin	10 mg/kg/day	High oxalate fed C57BL/6 mice	(68)
		ipragliflozin	4 mg/kg/day	BTBR *ob/ob* mice	(76)
Creatinine clearance	(-)	dapagliflozin	1 mg/kg/day	HFD fed Wistar rats	(63)
		ipragliflozin	0,3-3,0 mg/kg/day	STZ-BALB/c mice	(65)
	(+)	dapagliflozin	1 mg/kg/day	OLEFT rats	(73)
			2 mg/kg/day	STZ-Wistar rats	(82)
		ipragliflozin	1,0-3,0 mg/kg/day	UNX KK-Ay mice	(74)
				UNX STZ-ICR mice	(75)
		luseogliflozin	30 mg/kg/day	IR-C57BL/6 mice	(58)
	(=)	dapagliflozin	0,1-1,0 mg/kg/day	*db/db* mice	(60)
			1 mg/kg/day	*db/db* mice	(64)
				UNX *db/db* mice	(77)
		empagliflozin	30 mg/kg/day	BTBR *ob/ob* mice	(61)
				BTBR *ob/ob* mice + hypertension	(61)
		ipragliflozin	0,3-3,0 mg/kg/day	*db/db* mice	(65)
		tofogliflozin	5,0-15,0 mg/kg/day	*db/db* mice	(69)
Urine volume	(-)	ipragliflozin	0,3-3,0 mg/kg/day	*db/db* mice	(65)
		luseogliflozin	10 mg/kg/day	STZ-Dahl rats	(66)

Parameter	Effect	iSGLT2	Dosage	Experimental model	Reference
		tofogliflozin	5,0-15,0 mg/kg/day	*db/db* mice	(69)
	(+)	dapagliflozin	1 mg/kg/day	HFD fed Wistar rats	(63)
		ipragliflozin	3,0 mg/kg/day	UNX KK-Ay mice	(74)
	(=)	dapagliflozin	0,1-1,0 mg/kg/day	*db/db* mice	(60)
			1 mg/kg/day	*db/db* mice	(64)
				SNX Sprague Dawley rats	(72)
				UNX *db/db* mice	(77)
			2 mg/kg/day	STZ-Wistar rats	(82)
		empagliflozin	10 mg/kg/day	*db/db* mice	(84)
		luseogliflozin	30 mg/kg/day	IR-C57BL/6 mice	(58)
Proteinuria	(-)	ipragliflozin	1,0-3,0 mg/kg/day	UNX KK-Ay mice	(74)
			3,0 mg/kg/day	UNX STZ-ICR mice	(75)
	(=)	dapagliflozin	1 mg/kg/day	SNX Sprague Dawley rats	(80)
				SNX Sprague Dawley rats	(72)
		luseogliflozin	10 mg/kg/day	STZ-Dahl rats	(66)
				T2DN rats	(67)
Albuminuria	(-)	dapagliflozin	0,1-1,0 mg/kg/day	*db/db* mice	(60)
			1 mg/kg/day	HFD fed Wistar rats	(63)
				OLEFT rats	(73)
				UNX *db/db* mice	(77)
			2 mg/kg/day	STZ-Wistar rats	(82)
		empagliflozin	30 mg/kg/day	BTBR *ob/ob* mice	(61)
				BTBR *ob/ob* mice + hypertension	(61)
		ipragliflozin	0,3-3,0 mg/kg/day	STZ-BALB/c mice	(65)
			1,0-3,0 mg/kg/day	UNX KK-Ay mice	(74)
			3,0 mg/kg/day	*db/db* mice	(65)
				UNX STZ-ICR mice	(75)
		tofogliflozin	5,0-15,0 mg/kg/day	KK-Ay/Ta mice	(62)
	(+)	dapagliflozin	1 mg/kg/day	*db/db* mice	(64)
	(=)	empagliflozin	10 mg/kg/day	*db/db* mice	(84)
				STZ-Sprague Dawley rats	(70)
		ipragliflozin	4 mg/kg/day	BTBR *ob/ob* mice	(76)
Albumin/creatinine ratio	(-)	dapagliflozin	1 mg/kg/day	OLEFT rats	(73)
			5 mg/kg/day	WD fed C57BL/6 mice	(79)
		empagliflozin	70 mg/kg/day	Ins2+/Akita mice	(78)
		tofogliflozin	5,0-15,0 mg/kg/day	*db/db* mice	(69)
	(+)	dapagliflozin	1 mg/kg/day	*db/db* mice	(64)
	(=)	empagliflozin	10 mg/kg/day	STZ-eNOS knockout C57BL/6 mice	(85)
Urine urea	(=)	dapagliflozin	1 mg/kg/day	*db/db* mice	(64)
Filtered glucose load	(-)	empagliflozin	10 mg/kg/day	*db/db* mice	(84)
Glucose clearance	(+)	tofogliflozin	5,0-15,0 mg/kg/day	*db/db* mice	(69)
Urine glucose	(-)	dapagliflozin	0,1-1,0 mg/kg/day	*db/db* mice	(60)
	(+)	dapagliflozin	1 mg/kg/day	HFD fed Wistar rats	(63)
		ipragliflozin	0,1-3,0 mg/kg/day	UNX STZ-ICR mice	(75)
				UNX KK-Ay mice	(74)
		luseogliflozin	10 mg/kg/day	STZ-Dahl rats	(66)
				T2DN rats	(67)
	(=)	dapagliflozin	1 mg/kg/day	*db/db* mice	(64)
		empagliflozin	10 mg/kg/day	High oxalate fed C57BL/6 mice	(68)
				db/db mice	(84)
				STZ-eNOS knockout C57BL/6 mice	(85)
				STZ-Sprague Dawley rats	(70)
		ipragliflozin	4 mg/kg/day	BTBR *ob/ob* mice	(76)
		tofogliflozin	5,0-15,0 mg/kg/day	*db/db* mice	(69)
Urine sodium	(+)	dapagliflozin	1,5 mg/kg/day	UNX Protein-overload proteinuria C57BL/6 mice	(83)
Urine oxalate	(=)	empagliflozin	10 mg/kg/day	High oxalate fed C57BL/6 mice	(68)
Urine podocalyxin	(-)	ipragliflozin	1,0-3,0 mg/kg/day	UNX KK-Ay mice	(74)
			3,0 mg/kg/day	UNX STZ-ICR mice	(75)
Urine nephrin	(-)	ipragliflozin	1,0-3,0 mg/kg/day	UNX KK-Ay mice	(74)
			3,0 mg/kg/day	UNX STZ-ICR mice	(75)
		luseogliflozin	10 mg/kg/day	T2DN rats	(67)
Urine calcium	(=)	empagliflozin	10 mg/kg/day	High oxalate fed C57BL/6 mice	(68)
Urine osmolality	(=)	dapagliflozin	1 mg/kg/day	*db/db* mice	(64)
Plasmatic Cystatin C	(=)	empagliflozin	10 mg/kg/day	*db/db* mice	(84)
FABP	(-)	empagliflozin	10 mg/kg/day	STZ-Sprague Dawley rats	(70)

The effect column sums up the information available in all included studies. (-) indicates a statistically significant decrease in the parameter; (+) indicates a significant increase in the parameter; (=) indicates there was no significant differences in the parameter. FABP: Fatty acid-binding protein; HFD: High-fat diet; IR: Ischemia-reperfusion; SNX: Subtotal nephrectomy; STZ: Streptozotocin; UUO: Unilateral ureteric obstruction; UNX: Unilateral nephrectomy; WD: Western diet;

As would be expected from substances that inhibit glucose and sodium re-uptake, filtered glucose load was lower and urine sodium was higher in animals treated with iSGLT2, however only one study had relevant data for each of these parameters. Urinary glucose concentration had mixed outcomes, with the bigger percentage of experiments reporting no changes, while 5 experiments reported increased levels and 1 study reported lower levels of glucose in the urine of treated animals (Table 6).

Urinary podocalyxin and nephrin concentrations, biomarkers of glomerular injury, were decreased by iSGLT2 action in the trials in which they were evaluated. On the other hand, fatty acid-binding protein (FABP), a biomarker of tubular injury, was decreased by empagliflozin in the only trial where it was assessed (Table 6).

3.2.3. Kidney function (Tecidular markers)

Tissue biomarkers of kidney function, namely those indicative of AKI, glomerular injury, tubular injury and fibrotic processes, were amongst the selected indicators to evaluate potential mechanisms underlying iSGLT2 nephroprotection.

Table 7 - Effect of iSGLT2 on tecidular markers of kidney function

Parameter	Effect	iSGLT2	Dosage	Experimental model	Reference
Renal Cystatin C	(=)	dapagliflozin	1 mg/kg/day	Fructose fed STZ-Wistar rats	(71)
IGFBP7#	(=)	empagliflozin	10 mg/kg/day	High oxalate fed C57BL/6 mice	(68)
NGAL*	(-)	dapagliflozin	1 mg/kg/day	Fructose fed STZ-Wistar rats	(71)
NGAL#	(-)	dapagliflozin	1 mg/kg/day	HFD fed Wistar rats	(63)
	(=)	ipragliflozin	0,3-3,0 mg/kg/day	*db/db* mice	(65)
TIMP2*	(-)	empagliflozin	70 mg/kg/day	Ins2+/Akita mice	(78)
TIMP2#	(=)	empagliflozin	10 mg/kg/day	High oxalate fed C57BL/6 mice	(68)
Vanin 1*	(-)	dapagliflozin	1 mg/kg/day	Fructose fed STZ-Wistar rats	(71)
Nephrin*	(+)	dapagliflozin	1 mg/kg/day	Fructose fed STZ-Wistar rats	(71)
			1,5 mg/kg/day	UNX Protein-overload proteinuria C57BL/6 mice	(83)
			5 mg/kg/day	WD fed C57BL/6 mice	(79)
Nestin*	(+)	dapagliflozin	1,5 mg/kg/day	UNX Protein-overload proteinuria C57BL/6 mice	(83)
Synaptopodin*	(+)	dapagliflozin	5 mg/kg/day	WD fed C57BL/6 mice	(79)
	(+)	ipragliflozin	0,3-3,0 mg/kg/day	*db/db* mice	(65)
KIM1*	(-)	dapagliflozin	1 mg/kg/day	Fructose fed STZ-Wistar rats	(71)
		ipragliflozin	1,0-3,0 mg/kg/day	UNX KK-Ay mice	(74)
			3,0 mg/kg/day	UNX STZ-ICR mice	(75)
	(=)	empagliflozin	10 mg/kg/day	High oxalate fed C57BL/6 mice	(68)
				db/db mice	(84)
KIM1#	(-)	ipragliflozin	0,3-3,0 mg/kg/day	*db/db* mice	(65)
	(=)	empagliflozin	10 mg/kg/day	High oxalate fed C57BL/6 mice	(68)
NAG*	(-)	dapagliflozin	1 mg/kg/day	Fructose fed STZ-Wistar rats	(71)
		ipragliflozin	1,0-3,0 mg/kg/day	UNX KK-Ay mice	(74)
			3,0 mg/kg/day	UNX STZ-ICR mice	(75)
		tofogliflozin	5,0-15,0 mg/kg/day	KK-Ay/Ta mice	(62)
Slc34a1#	(+)	ipragliflozin	3,0 mg/kg/day	*db/db* mice	(65)
Klotho*	(+)	empagliflozin	10 mg/kg/day	UUO Wistar rats	(81)

*The effect column sums up the information available in all included studies. # indicates a parameter assessed by mRNA expression levels; * indicates a parameter assessed by protein expression levels; (-) indicates a statistically significant decrease in the parameter; (+) indicates a significant increase in the parameter; (=) indicates there was no significant differences in the parameter. HFD: High-fat diet; IGFBP7: Insulin-like growth factor-binding protein 7; KIM1: Kidney injury molecule-1; NAG: N-acetil-β-D-glicosaminidase; NGAL: Neutrophil gelatinase-associated lipocalin; SNX: Subtotal nephrectomy; STZ: Streptozotocin; THBS1: Thrombospondin 1; TNC: Tenascin C; UNX: Unilateral nephrectomy; UUO: Unilateral ureteric obstruction; WD: Western diet;*

In studies where NGAL, tissue inhibitor of metalloproteinases 2 (TIMP2) and vanin 1 protein expressions were assessed, treatment with iSGLT2 elicited a significant reduction of their values. Insulin-like growth factor-binding protein 7 (IGFBP7) was the only AKI indicator that did not have any report of relevant changes due to an iSGLT2 action (Table 7).

As far as glomerular and tubular damage were concerned, evaluation of histopathological features was commonly preferred. Glomerular injury was evaluated through 3 different markers. Tissue levels of nephrin, nestin and synaptopodin were significantly raised when SGLT2 inhibition was applied. Tubular injury was directly evaluated through quantification of 3 different markers. The enzyme NAG was measured in 4 rodent models. In all experiments, treatment with iSGLT2 substances reduced the concentration of this tubular injury marker. KIM1 protein levels were reduced in the majority of studies, whereas mRNA levels of Slc34a1 (gene responsible for coding sodium-dependent phosphate transporter 2A) were elevated in a single study (Table 7).

3.3. Influence of iSGLT2 on cellular and molecular mechanisms underlying renal injury

Documented effects of iSGLT2 action on the intertwined processes of inflammation, oxidative stress and cellular mechanisms recruited upon injury are detailed in the following sub-sections.

3.3.1. Oxidative stress

Products of oxidative stress 3-nitrotyrosine (3NT), 8OHdG and MDA were reduced in the presence of iSGLT2 treatment across all reports included in present study. With at least 3 experimental models evaluating each oxidative stress marker, it is noteworthy the uniformity of the observed outcomes, suggesting a strong correlation between iSGLT2 treatment and a reduction in ROS. Likewise, levels of hydrogen peroxide significantly dropped when dapagliflozin was administered to OLEFT rats (Table 8).

It is likely that the described reduction in oxidative stress products may be linked to a similar reduction observed in enzymes responsible for oxidative stress processes. iSGLT2 drugs significantly reduced protein expression of superoxide generator enzymes NADPH oxidase isoforms 2 (Nox2) and 4 (Nox4) in all observed experiments. Furthermore, inducible nitric oxide synthase (iNOS) was significantly reduced following dapagliflozin treatment in an HFD fed Wistar rat experimental model, and endothelial nitric oxide synthase (eNOS) was augmented by empagliflozin in a *db/db* mice model, showcasing a reduction in oxidative stress insults in both experiments (Table 8).

In the field of antioxidant enzymes, dapagliflozin was able to significantly elevate the levels of the hydrogen peroxide decomposing enzyme catalase and of superoxide dismutase isoenzyme 2 (SOD2) in one experimental model of OLEFT rats. Superoxide dismutase isoenzyme 1 (SOD1) was assessed in 5 different experimental models and had mixed results, with a significant elevation in the enzyme levels of 3 treated animal models along with a significant reduction in the enzyme expression of 1 treated animal model and 1 treated *in vitro* model (Table 8).

Antioxidant enzyme glutathione peroxidase (GSH-Px) was also elevated following treatment with SGLT2 inhibitors in 2 different studies. However, glutathione (GSH) and glutathione disulfide (GSSG) had more modest results, with GSH being elevated in one treated model of fructose fed and STZ injured Wistar rats, but both GSH and GSSG had no changes in genetically obese BTBR *ob/ob* mice upon iSGLT2 treatment (Table 8).

Finally, some studies calculated total antioxidant capacity (TAC), an indicator of an organism ability to react to oxidative injury, and total oxidant status (TOS), an indicator of the overall oxidative status of an organism. In both markers, iSGLT2 treatment was linked with a protective role upon oxidative stress (Table 8).

A robust influence of iSGLT2 substances on AGEs formation was observed. Particularly, iSGLT2 were able to significantly reduce AGEs modified protein levels, the levels of receptors for AGEs (RAGE) and of RAGE ligand high mobility group box 1 (HMGB1). Also, in the presence of dapagliflozin, the levels of soluble form of RAGE (sRAGE) were increased relative to groups without treatment.

3.3.2. Inflammation

Due to the relevance of inflammation and oxidative-stress processes on renal disease progression, a large array of related biomarkers was studied in the reports included in this review.

Regarding cytokines, the pro-inflammatory interleukin 1 (IL1) and interleukin 6 (IL6) were reduced in all experiments when treatment with iSGLT2 was applied (Table 8).

Chemokine ligand 2 (CCL2) protein concentration was also significantly reduced in the presence of an iSGLT2, in a total of 6 experimental models. Another chemokine, the chemokine ligand 5 (CCL5) was quantified in a BTBR *ob/ob* mice experimental model but remained unchanged in the presence of empagliflozin (Table 8).

Furthermore, and although responsible for a multitude of biological processes, TGFβ was primarily investigated due to its role in immune regulation and inflammatory processes.

Interestingly, TGFβ protein expression was reduced upon iSGLT2 treatment in 4 *in vivo* models and remained unchanged in 1. Another inflammatory cytokine, tumor necrosis factor alfa (TNFα), exhibited a reduction in their levels in 4 *in vivo* studies when animals were treated with an iSGLT2. Finally, osteopontin, a protein with immunologic cytokine properties, was the only cytokine with no protein quantification, but revealed a significant depletion in mRNA levels when dapagliflozin was present in 3 experimental models. Overall, iSGLT2 were largely associated with a reduction of inflammatory cytokines levels (Table 8).

Table 8 - Effect of iSGLT2 on inflammation, oxidative stress and AGEs

Parameter	Effect	iSGLT2	Dosage	Experimental model	Reference
IL1*	(-)	ipragliflozin	1,0-3,0 mg/kg/day	UNX KK-Ay mice	(74)
			3,0 mg/kg/day	UNX STZ-ICR mice	(75)
		dapagliflozin	1 mg/kg/day	HFD fed Wistar rats	(63)
IL6*	(-)	ipragliflozin	1,0-3,0 mg/kg/day	UNX KK-Ay mice	(74)
			3,0 mg/kg/day	UNX STZ-ICR mice	(75)
		empagliflozin	100-500 nM	HK2 cells +HG	(54)
IL6#	(=)	empagliflozin	30 mg/kg/day	BTBR *ob/ob* mice	(61)
CCL2*	(-)	dapagliflozin	1 mg/kg/day	Fructose fed STZ-Wistar rats	(71)
			10-100 µM	HK2 cells +HG	(56)
		ipragliflozin	1,0-3,0 mg/kg/day	UNX KK-Ay mice	(74)
			3,0 mg/kg/day	UNX STZ-ICR mice	(75)
	(-)	dapagliflozin	1 mg/kg/day	UNX *db/db* mice	(77)
		empagliflozin	70 mg/kg/day	Ins2+/Akita mice	(78)
CCL2#	(-)	dapagliflozin	1,0 mg/kg/day	*db/db* mice	(60)
			20,0 µM	mProx24 cells + HG	(60)
		empagliflozin	10 mg/kg/day	STZ-Sprague Dawley rats	(70)
	(-)	dapagliflozin	5 mg/kg/day	WD fed C57BL/6 mice	(79)
	(=)	empagliflozin	10 mg/kg/day	STZ-eNOS knockout C57BL/6 mice	(85)
			30 mg/kg/day	BTBR *ob/ob* mice	(61)
		ipragliflozin	4 mg/kg/day	BTBR *ob/ob* mice	(76)
CCL5#	(=)	empagliflozin	30 mg/kg/day	BTBR *ob/ob* mice	(61)
TGFβ*	(-)	dapagliflozin	1 mg/kg/day	Fructose fed STZ-Wistar rats	(71)
			2 mg/kg/day	STZ-Wistar rats	(82)
			1 mg/kg/day	HFD fed Wistar rats	(63)
		empagliflozin	10 mg/kg/day	UUO Wistar rats	(81)
	(=)	empagliflozin	10 mg/kg/day	High oxalate fed C57BL/6 mice	(68)
TGFβ#	(-)	dapagliflozin	1 mg/kg/day	UNX *db/db* mice	(77)
				db/db mice	(60)
		empagliflozin	10 mg/kg/day	*db/db* mice	(84)
				STZ-Sprague Dawley rats	(70)
		luseogliflozin	30 mg/kg/day	IR-C57BL/6 mice	(58)
	(=)	empagliflozin	10 mg/kg/day	STZ-eNOS knockout C57BL/6 mice	(85)
TNFα-R1*	(-)	dapagliflozin	1 mg/kg/day	HFD fed Wistar rats	(63)
TNFα*	(-)	dapagliflozin	1 mg/kg/day	Fructose fed STZ-Wistar rats	(71)
				HFD fed Wistar rats	(63)
		ipragliflozin	1,0-3,0 mg/kg/day	UNX KK-Ay mice	(74)
			3,0 mg/kg/day	UNX STZ-ICR mice	(75)
TNFα#	(=)	empagliflozin	10 mg/kg/day	High oxalate fed C57BL/6 mice	(68)
osteopontin#	(-)	dapagliflozin	1,0 mg/kg/day	*db/db* mice	(60)
			20,0 µM	mProx24 cells + HG	(60)
			5 mg/kg/day	WD fed C57BL/6 mice	(79)
ICAM1*	(-)	dapagliflozin	10-100 µM	HK2 cells +HG	(56)
ICAM1#	(-)	dapagliflozin	0,1-1,0 mg/kg/day	*db/db* mice	(60)
		empagliflozin	10 mg/kg/day	STZ-Sprague Dawley rats	(70)
	(-)	dapagliflozin	5 mg/kg/day	WD fed C57BL/6 mice	(79)
C-Reactive protein*	(-)	ipragliflozin	1,0-3,0 mg/kg/day	UNX KK-Ay mice	(74)
			3,0 mg/kg/day	UNX STZ-ICR mice	(75)
CD11c*	(-)	dapagliflozin	1,0 mg/kg/day	*db/db* mice	(60)
CD14*	(-)	dapagliflozin	0,1-1,0 mg/kg/day	*db/db* mice	(60)
	(-)	empagliflozin	70 mg/kg/day	Ins2+/Akita mice	(78)
CD14#	(=)	empagliflozin	10 mg/kg/day	*db/db* mice	(84)

Parameter	Effect	iSGLT2	Dosage	Experimental model	Reference
CD206*	(=)	dapagliflozin	0,1-1,0 mg/kg/day	*db/db* mice	(60)
CD68*	(-)	dapagliflozin	5 mg/kg/day	WD fed C57BL/6 mice	(79)
TLR2*	(=)	empagliflozin	10 mg/kg/day	STZ-eNOS knockout C57BL/6 mice	(85)
TLR2#	(-)	dapagliflozin	5 mg/kg/day	WD fed C57BL/6 mice	(79)
TLR4*	(-)	empagliflozin	10 mg/kg/day	UUO Wistar rats	(81)
	(-)	empagliflozin	100-500 nM	HK2 cells +HG	(54)
NLRP3#	(=)	empagliflozin	10 mg/kg/day	High oxalate fed C57BL/6 mice	(68)
COX2*	(-)	dapagliflozin	1 mg/kg/day	HFD fed Wistar rats	(63)
3NT	(-)	empagliflozin	10 mg/kg/day	*db/db* mice	(59)
		ipragliflozin	0,3-3,0 mg/kg/day	*db/db* mice	(65)
				STZ-BALB/c mice	(65)
8OHdG	(-)	dapagliflozin	1 mg/kg/day	OLEFT rats	(73)
		empagliflozin	10 mg/kg/day	STZ-Sprague Dawley rats	(70)
		ipragliflozin	10 mg/kg/day	HFD fed C57BL/6 mice	(57)
			3,0 mg/kg/day	*db/db* mice	(65)
				STZ-BALB/c mice	(65)
MDA	(-)	dapagliflozin	1 mg/kg/day	Fructose fed STZ-Wistar rats	(71)
				HFD fed Wistar rats	(63)
				OLEFT rats	(73)
				UNX *db/db* mice	(77)
			10-100 µM	HK2 cells +HG	(56)
			2 mg/kg/day	STZ-Wistar rats	(82)
		ipragliflozin	4 mg/kg/day	BTBR *ob/ob* mice	(76)
Hydrogen peroxide	(-)	dapagliflozin	1 mg/kg/day	OLEFT rats	(73)
Nox2*	(-)	dapagliflozin	1 mg/kg/day	UNX *db/db* mice	(77)
				db/db mice	(60)
			5 mg/kg/day	WD fed C57BL/6 mice	(79)
Nox2#	(-)	dapagliflozin	20,0 µM	mProx24 cells + HG	(60)
			5 mg/kg/day	WD fed C57BL/6 mice	(79)
Nox4*	(-)	dapagliflozin	1 mg/kg/day	UNX *db/db* mice	(77)
		ipragliflozin	0,3-3,0 mg/kg/day	*db/db* mice	(65)
iNOS*	(-)	dapagliflozin	1 mg/kg/day	HFD fed Wistar rats	(63)
eNOS*	(+)	empagliflozin	10 mg/kg/day	*db/db* mice	(59)
Catalase*	(+)	dapagliflozin	1 mg/kg/day	OLEFT rats	(73)
SOD1*	(-)	dapagliflozin	1 mg/kg/day	HFD fed Wistar rats	(63)
			10-100 µM	HK2 cells +HG	(56)
	(+)	dapagliflozin	1 mg/kg/day	OLEFT rats	(73)
				Fructose fed STZ-Wistar rats	(71)
			2 mg/kg/day	STZ-Wistar rats	(82)
SOD2*	(+)	dapagliflozin	1 mg/kg/day	OLEFT rats	(73)
Heme oxygenase 1*	(=)	empagliflozin	70 mg/kg/day	Ins2+/Akita mice	(78)
GSH*	(+)	dapagliflozin	1 mg/kg/day	Fructose fed STZ-Wistar rats	(71)
	(=)	ipragliflozin	4 mg/kg/day	BTBR *ob/ob* mice	(76)
GSH-Px*	(+)	dapagliflozin	1 mg/kg/day	HFD fed Wistar rats	(63)
			2 mg/kg/day	STZ-Wistar rats	(82)
GSSG*	(=)	ipragliflozin	4 mg/kg/day	BTBR *ob/ob* mice	(76)
TAC	(+)	dapagliflozin	2 mg/kg/day	STZ-Wistar rats	(82)
TOS	(-)	dapagliflozin	0,1-1,0 mg/kg/day	*db/db* mice	(60)
			0,2-20,0 µM	mProx24 cells + HG	(60)
			2 mg/kg/day	STZ-Wistar rats	(82)
AGE-modified proteins	(-)	empagliflozin	10 mg/kg/day	*db/db* mice	(59)
				STZ-Sprague Dawley rats	(70)
HMGB1*	(-)	dapagliflozin	10-100 µM	HK2 cells +HG	(56)
RAGE*	(-)	dapagliflozin	10-100 µM	HK2 cells +HG	(56)
		empagliflozin	10 mg/kg/day	STZ-Sprague Dawley rats	(70)
RAGE#	(-)	empagliflozin	10 mg/kg/day	STZ-Sprague Dawley rats	(70)
sRAGE*	(+)	dapagliflozin	2 mg/kg/day	STZ-Wistar rats	(82)

*The effect column sums up the information available in all included studies. # indicates a parameter assessed by mRNA expression levels; * indicates a parameter assessed by protein expression levels; (-) indicates a statistically significant decrease in the parameter; (+) indicates a significant increase in the parameter; (=) indicates there was no significant differences in the parameter; AGE: Advanced glycation end products; CCL2: Chemokine ligand 2; CCL5: Chemokine ligand 5; CD11c: Cluster of differentiation 11c; CD14: Cluster of differentiation 14; CD206: Cluster of differentiation 206; CD68: Cluster of differentiation 68; COX2: Cyclooxygenase 2; eNOS: Endothelial nitric oxide synthase; GSH: Glutathione; GSH-Px: Glutathione peroxidase; GSSG: Glutathione disulfide; HFD: High-fat diet; HK2: Human kidney 2 proximal tubule; HMGB1: High mobility group box 1; ICAM1: Intercellular adhesion molecule 1; IL1: Interleukin 1; IL6: Interleukin 6; iNOS: Inducible nitric oxide synthase; MDA: Malondialdehyde; Nox2: NADPH oxidase isoform 2; Nox4: NADPH oxidase isoform 4; RAGE: Receptors for advanced glycation end products; SNX: Subtotal nephrectomy; SOD1: Superoxide dismutase isoenzyme 1; SOD2: Superoxide dismutase isoenzyme 2; sRAGE: Soluble receptor for advanced glycation end products; STZ: Streptozotocin; TAC: Total antioxidant capacity; TGFß: Transforming growth factor beta; TLR2: Toll-like receptor 2; TLR4: Toll-like receptor 4; TNFα: Tumor necrosis factor alfa; TOS: Total oxidant status; UUO: Unilateral ureteric obstruction; UNX: Unilateral nephrectomy; WD: Western diet; 3NT; 3-Nitrotyrosine; 8OHdG: 8-hydroxydeoxyguanosine;*

Beside cytokines, inflammatory processes were also evaluated through surface proteins, enzymes and related proteins. Dapagliflozin significantly lowered intercellular adhesion molecule 1 (ICAM1)

protein levels as well as cluster of differentiation 14 (CD14), a co-receptor mainly expressed in macrophages. Another three members of the cluster of differentiation family, cluster of differentiation 11c (CD11c), CD68 and cluster of differentiation 206 (CD206), all markers of macrophages, were decreased in the presence of an iSGLT2 (Table 8).

Toll-like receptors 2 (TLR2) and 4 (TLR4) belonging to the innate immune system were also assessed. Only TLR4 experienced significant changes, being lower in two experimental models treated with iSGLT2. Similarly, a reduction of the expression of the enzyme cyclooxygenase 2 (COX2) was observed in one study of high-fat diet (HFD) fed Wistar rats treated with dapagliflozin. Also, the inflammatory C-reactive protein was lowered in the presence of ipragliflozin in two reports (Table 8).

3.3.3. Fibrosis

Fibrotic markers were thoroughly evaluated with a large array of parameters (21 in total) assessed. Hereon, we highlight those that were repeatedly assessed and/or those displaying steady results among multiple experimental models. It should be noted that no evidence of fibrotic marker worsening was noted in the presence of any iSGLT2.

Table 9 - Effect of iSGLT2 on fibrotic markers

Parameter	Effect	iSGLT2	Dosage	Experimental model	Reference
Total collagen*	(-)	dapagliflozin	1 mg/kg/day	Fructose fed STZ-Wistar rats	(71)
	(=)	empagliflozin	10 mg/kg/day	STZ-eNOS knockout C57BL/6 mice	(85)
Collagen I*	(-)	dapagliflozin	10-100 µM	HK2 cells +HG	(56)
		empagliflozin	10 mg/kg/day	*db/db* mice	(59)
	(=)	dapagliflozin	1 mg/kg/day	SNX Sprague Dawley rats	(80)
		empagliflozin	10 mg/kg/day	High oxalate fed C57BL/6 mice	(68)
				High oxalate fed C57BL/6 mice	(68)
Collagen I#	(=)	ipragliflozin	4 mg/kg/day	BTBR *ob/ob* mice	(76)
Collagen III*	(-)	empagliflozin	10 mg/kg/day	*db/db* mice	(59)
Collagen IV*	(-)	dapagliflozin	0,1-1,0 mg/kg/day	*db/db* mice	(60)
			1 mg/kg/day	HFD fed Wistar rats	(63)
				OLEFT rats	(73)
				UNX *db/db* mice	(77)
			5 mg/kg/day	WD fed C57BL/6 mice	(79)
		empagliflozin	100-500 nM	HK2 cells +HG	(54)
	(=)	dapagliflozin	1 mg/kg/day	SNX Sprague Dawley rats	(72)
		ipragliflozin	4 mg/kg/day	BTBR *ob/ob* mice	(76)
Collagen IV#	(-)	dapagliflozin	1 mg/kg/day	UNX *db/db* mice	(77)
	(=)	dapagliflozin	1 mg/kg/day	SNX Sprague Dawley rats	(80)
		empagliflozin	10 mg/kg/day	*db/db* mice	(84)
Ctgf*	(-)	empagliflozin	10 mg/kg/day	UUO Wistar rats	(81)
Ctgf#	(-)	empagliflozin	10 mg/kg/day	STZ-Sprague Dawley rats	(70)
	(=)	empagliflozin	10 mg/kg/day	*db/db* mice	(84)
F-actin*	(-)	dapagliflozin	1,5 mg/kg/day	UNX Protein-overload proteinuria C57BL/6 mice	(83)
Fibronectin*	(-)	dapagliflozin	1 mg/kg/day	UNX *db/db* mice	(77)
			10-100 µM	HK2 cells +HG	(56)
			5 mg/kg/day	WD fed C57BL/6 mice	(79)
		empagliflozin	10 mg/kg/day	*db/db* mice	(59)
				UUO Wistar rats	(81)
	(=)	empagliflozin	10 mg/kg/day	High oxalate fed C57BL/6 mice	(68)
				STZ-eNOS knockout C57BL/6 mice	(85)
Fibronectin#	(-)	dapagliflozin	1 mg/kg/day	UNX *db/db* mice	(77)

Parameter	Effect	iSGLT2	Dosage	Experimental model	Reference
		empagliflozin	10 mg/kg/day	*db/db* mice	(84)
	(=)	empagliflozin	10 mg/kg/day	STZ-eNOS knockout C57BL/6 mice	(85)
FSP1*	(=)	empagliflozin	10 mg/kg/day	High oxalate fed C57BL/6 mice	(68)
Hydroxyproline*	(-)	dapagliflozin	1 mg/kg/day	OLEFT rats	(73)
PAI1#	(-)	dapagliflozin	1 mg/kg/day	UNX *db/db* mice	(77)
		empagliflozin	10 mg/kg/day	STZ-Sprague Dawley rats	(70)
RECK*	(+)	empagliflozin	10 mg/kg/day	*db/db* mice	(59)
			500 nM	HK2 cells +HG	(59)
Phospho-Smad2	(=)	dapagliflozin	1 mg/kg/day	SNX Sprague Dawley rats	(80)
PDGFB*	(-)	canagliflozin	500 nM	HK2 cells + TGFβ	(53)
		empagliflozin	500 nM	HK2 cells + TGFβ	(53)
PDGFB#	(=)	canagliflozin	500 nM	HK2 cells + TGFβ	(53)
				RPTEC cells + TGFβ	(53)
		empagliflozin	500 nM	HK2 cells + TGFβ	(53)
				RPTEC cells + TGFβ	(53)
THBS1*	(-)	canagliflozin	500 nM	HK2 cells + TGFβ	(53)
		empagliflozin	500 nM	HK2 cells + TGFβ	(53)
THBS1#	(-)	canagliflozin	500 nM	HK2 cells + TGFβ	(53)
				RPTEC cells + TGFβ	(53)
		empagliflozin	500 nM	HK2 cells + TGFβ	(53)
				RPTEC cells + TGFβ	(53)
TNC*	(-)	canagliflozin	500 nM	HK2 cells + TGFβ	(53)
		empagliflozin	500 nM	HK2 cells + TGFβ	(53)
TNC#	(-)	canagliflozin	500 nM	HK2 cells + TGFβ	(53)
				RPTEC cells + TGFβ	(53)
		empagliflozin	500 nM	HK2 cells + TGFβ	(53)
				RPTEC cells + TGFβ	(53)
Wnt1*	(-)	empagliflozin	10 mg/kg/day	UUO Wistar rats	(81)
α-Actinin-4	(+)	dapagliflozin	1,5 mg/kg/day	UNX Protein-overload proteinuria C57BL/6 mice	(83)
αSMA*	(-)	dapagliflozin	1 mg/kg/day	Fructose fed STZ-Wistar rats	(71)
		empagliflozin	10 mg/kg/day	UUO Wistar rats	(81)
	(=)	empagliflozin	10 mg/kg/day	High oxalate fed C57BL/6 mice	(68)
αSMA#	(=)	ipragliflozin	4 mg/kg/day	BTBR *ob/ob* mice	(76)
β1-Integrin*	(+)	dapagliflozin	1,5 mg/kg/day	UNX Protein-overload proteinuria C57BL/6 mice	(83)

*The effect column sums up the information available in all included studies. # indicates a parameter assessed by mRNA expression levels; * indicates a parameter assessed by protein expression levels; (-) indicates a statistically significant decrease in the parameter; (+) indicates a significant increase in the parameter; (=) indicates there was no significant differences in the parameter. Ctgf: Connective tissue growth factor; FSP1: Fibroblast marker; HFD: High-fat diet; HK2: Human kidney 2 proximal tubule; IGFBP7: Insulin-like growth factor-binding protein 7; PAI1: Plasminogen activator inhibitor-1; PDGFB: Platelet-derived growth factor subunit-B; RECK: Reversion-inducing-cysteine-rich protein; RPTEC: Renal proximal tubule epithelial cells; SNX: Subtotal nephrectomy; STZ: Streptozotocin; THBS1: Thrombospondin 1; TNC: Tenascin C; UNX: Unilateral nephrectomy; UUO: Unilateral ureteric obstruction; WD: Western diet; αSMA: alfa-smooth muscle actin*

Starting with collagen IV, the most investigated isoform of collagen, 75% of studies reported a down-regulation of collagen IV protein levels. Collagen I and total collagen also had reported evidence of down-regulation with iSGLT2 treatment, but no more than 50% of studies focused this outcome. Collagen III was only reported in 1 study, in which empagliflozin significantly reduced their expression. Furthermore, fibronectin expression was also widely reduced in the studies included in this review, as 5 out 7 experiments reported a significant reduction in their protein levels. Also noteworthy, one study evaluated the impact of canagliflozin and empagliflozin *in vitro* on the expression of 3 proteins of interest in tubulointerstitial fibrotic process: platelet-derived growth factor subunit B (PDGFB), thrombospondin 1 (THBS1) and tenascin C (TNC). All protein levels were down-regulated by both iSGLT2 in 2 distinct tubular cell lines. Lastly, αSMA was lower in treated rats in 2 experiments but failed to achieve the same outcome in an experimental model replicated in mice (Table 9).

3.3.4. Cellular response to stress

Three relevant mechanisms of cellular response to stress are apoptosis, autophagy and cellular senescence. Herein, we express the relevant data concerning these mechanisms collected from the studies included in the present review.

Quantification of apoptotic cells was done through TUNEL assay in 3 experiments, in all of which dapagliflozin had a significant impact in lowering the numbers of apoptotic cells in disease model animals (Table 10).

Mitochondrial morphology, an indicator of cellular apoptotic response, was evaluated in an experimental model of HFD fed C57BL/6 mice. In this experiment, ipragliflozin successfully led to an amelioration in mitochondrial morphology by reducing the number of fragmented and rounded mitochondria, indicating a reduction in the activation of apoptotic pathways. The same study evaluated both *in vivo* and *in vitro* the effects of ipragliflozin in mitochondrial fusion proteins, Mfn2 and dynamin family GTPase Opa1. Both molecules were upregulated in the presence of iSGLT2 drugs. In the same context, the mitochondrial anti-apoptotic protein B-cell lymphoma 2 (Bcl-2) and the pro-apoptotic protein Bcl-2-associated X (Bax) were investigated. Interestingly, both proteins and their calculated ratio seemed to benefit from iSGLT2 treatment, indicating a reduction in apoptosis activation. Additional apoptotic mediators were considered, and in an experimental model of HFD fed Wistar rats, binding immunoglobulin protein (BIP), cytochrome C, calpain-2 and CCAAT/enhancer-binding protein homologous protein (CHOP) levels were assessed. SGLT2 inhibitor dapagliflozin caused a statistically significant reduction in these mediators, suggesting a link with the decline in apoptotic cascades activation. Further reinforcing this assumption, various members of the caspase superfamily, namely Caspase-12, Cleaved caspase-3 and Caspase-7, displayed decreased protein levels when iSGLT2 treatment was administered (Table 10).

Table 8 - Effect of iSGLT2 on apoptosis, autophagy and cellular senescence

Parameter	Effect	iSGLT2	Dosage	Experimental model	Reference
Apoptotic cells	(-)	dapagliflozin	1,0 mg/kg/day	*db/db* mice	(60)
				HFD fed Wistar rats	(63)
			10 mg/kg/day	IR-C57BL/6 mice	(55)
Mitochondrial morphology	(+)	ipragliflozin	10 mg/kg/day	HFD fed C57BL/6 mice	(57)
Mfn2	(+)	ipragliflozin	10 mg/kg/day	HFD fed C57BL/6 mice	(57)
			10 nmol/L	HK2 cells + Palmitate	(57)
Opa1	(+)	ipragliflozin	10 mg/kg/day	HFD fed C57BL/6 mice	(57)
			10 nmol/L	HK2 cells + Palmitate	(57)
Drp1	(=)	ipragliflozin	10 mg/kg/day	HFD fed C57BL/6 mice	(57)
Bax*	(-)	dapagliflozin	1 mg/kg/day	HFD fed Wistar rats	(63)
			1-10 µM	HK2 cells + Hypoxia	(55)
			10 mg/kg/day	IR-C57BL/6 mice	(55)
Bax#	(-)	dapagliflozin	1,0 mg/kg/day	*db/db* mice	(60)
Bcl2*	(+)	dapagliflozin	1 mg/kg/day	HFD fed Wistar rats	(63)

Parameter	Effect	iSGLT2	Dosage	Experimental model	Reference
			10 mg/kg/day	IR-C57BL/6 mice	(55)
Bax/Bcl2 ratio	(-)	dapagliflozin	1-10 µM	HK2 cells + Hypoxia	(55)
			10 mg/kg/day	IR-C57BL/6 mice	(55)
Cytochrome C	(-)	dapagliflozin	1 mg/kg/day	HFD fed Wistar rats	(63)
CHOP	(-)	dapagliflozin	1 mg/kg/day	HFD fed Wistar rats	(63)
Calpain 2	(-)	dapagliflozin	1 mg/kg/day	HFD fed Wistar rats	(63)
Caspase-12*	(-)	dapagliflozin	1 mg/kg/day	HFD fed Wistar rats	(63)
Caspase-12#	(-)	dapagliflozin	1,0 mg/kg/day	*db/db* mice	(60)
Cleaved caspase-3*	(-)	dapagliflozin	1 mg/kg/day	HFD fed Wistar rats	(63)
Caspase-7*	(-)	dapagliflozin	1 mg/kg/day	Fructose fed STZ-Wistar rats	(71)
HIF1	(+)	dapagliflozin	10 mg/kg/day	IR-C57BL/6 mice	(55)
			5-10 µM	HK2 cells + Hypoxia	(55)
pAMPK	(=)	dapagliflozin	1-10 µM	HK2 cells + Hypoxia	(55)
pERK	(=)	dapagliflozin	1-10 µM	HK2 cells + Hypoxia	(55)
PARP	(-)	dapagliflozin	1-10 µM	HK2 cells + Hypoxia	(55)
			10 mg/kg/day	IR-C57BL/6 mice	(55)
BIP	(-)	dapagliflozin	1 mg/kg/day	HFD fed Wistar rats	(63)
Sirtuin1	(=)	ipragliflozin	4 mg/kg/day	BTBR *ob/ob* mice	(76)
p21	(=)	empagliflozin	70 mg/kg/day	Ins2+/Akita mice	(78)
p27	(-)	empagliflozin	70 mg/kg/day	Ins2+/Akita mice	(78)

*The effect column sums up the information available in all included studies. # indicates a parameter assessed by mRNA expression levels; * indicates a parameter assessed by protein expression levels; (-) indicates a statistically significant decrease in the parameter; (+) indicates a significant increase in the parameter; (=) indicates there was no significant differences in the parameter; Bax: Bcl-2-associated X; Bcl-2: B-cell lymphoma 2; BIP: Binding immunoglobulin protein; CHOP: CCAAT/enhancer-binding protein homologous proteinDrp1: Dynamin related protein 1; HFD: High-fat diet; HIF1: Hypoxia-inducible factor 1; HK2: Human kidney 2 proximal tubule; IR: Ischemia-reperfusion; Mfn2: Mitofusin 2; Opa1: Optic atrophy 1; PARP: poly-ADP-ribose polymerase*

Hypoxia is one amongst a multitude of insults that may induce apoptotic pathways. Thus, one study investigated the *in vivo* and *in vitro* influence of dapagliflozin on the expression of the hypoxia-inducible factor 1 (HIF1), a protein responsible for regulating cellular adaptive mechanisms in hypoxic conditions. In both experiments, dapagliflozin significantly contributed to the elevation of HIF1 levels, indicating a protective ability towards hypoxia-induced apoptosis (Table 10).

Autophagy regulation by iSGLT2 was minimally evaluated, with the corresponding results from the only study that directly tackled this mechanism showing that the autophagy regulator sirtuin1 was not changed in the presence of an iSGLT2 (Table 10).

Two members of the cyclin-dependent kinases family, p21 and p27, were evaluated in one study with the intent of evaluating the impact of iSGLT2 on cellular senescence. Only the latter molecule had a significant reduction when an iSGLT2 was administered (Table 10).

4. Discussion

Cardiovascular safety trials CANVAS(86), EMPA-REG(87) and DECLARE-TIMI 58(88) have shown beneficial effects on kidney protection, however, since the initial goal was to enroll diabetic patients at high cardiovascular risk, these studies may have included relatively few patients with renal diseases. CREDENCE(89) trial targeted this specific cohort, evidencing that diabetic patients taking SGLT2 inhibitor had reduced progression to end-stage renal disease, increased glomerular functions, and reduced death from renal causes. Clinical impact of iSGLT2 treatment in both diabetic and non-diabetic CKD is currently being evaluated in the DAPA-CKD trial (ClinicalTrials.gov Identifier: NCT03036150). In the present study, we proposed to dive into pre-clinical data and collect valid experimental evidence to better understand the range of mechanisms underlying iSGLT2 renoprotection. A resume of the main findings of present thesis is now presented, as follows:

4.1.1. Body and fat weight

Alongside the large majority of studies reporting no relevant differences in body weight, there were some conflicting results among experiments. Within clinical context, iSGLT2 treatment has been associated with body weight reduction.(90) Nevertheless, conflicting observations are pinpointed in the studies enrolled in this review with some experimental evidence showing a lack of effect in body weight reduction in diabetic rodent models. Since former works all display renoprotective effects upon iSGLT2 treatments, it is reasonable to suspect that iSGLT2-derived renoprotection may occur irrespectively of body weight reduction.

4.1.2. Metabolic profile

As expected regarding their mechanism of action and clinical evidence, metabolic profile was largely ameliorated in rodent diabetic models treated with SGLT2 inhibitors.(14,91) iSGLT2 ability to reduce plasma glucose was observed in almost every studies, with such evidence reported on both diabetic nephropathy and CKD models. Plasma glucose reduction has only failed in experiments with short duration (model of AKI).(68) Accordingly, HbA1c was reduced in every study, a logical consequence of plasmatic glucose reduction that paralleled in those experiments. With glycemia reduction, it is expected a plummeting of plasmatic insulin, which was observed in almost every experiment.

Insulin resistance, plasmatic levels of leptin and FGF21 (indicators of insulin resistance), plasmatic cholesterol and plasmatic triglycerides, risk factors of T2DM, were lowered in animals treated

with SGLT2 inhibitors. This was registered in models of diabetic nephropathy which is in line with the current clinical evidence.(92) Increased glucose/insulin tolerance were widely reported in animals treated with iSGLT2 drugs, which is in strict accordance with human evidence available.(93)

Interestingly, an exception among the collected results was observed in an experimental model of *db/db* mice treated with dapagliflozin for 12 weeks. This work reported that glucose/insulin tolerance did not changed upon iSGLT2 treatment, together with a worsened pyruvate tolerance. Alongside, plasmatic glucose was lowered and activation of gluconeogenesis was amplified, as supported by expression of gluconeogenic enzymes G6P and Pck1. This evidence points toward an imbalance in cellular glucose uptake that ultimately contributed to an exacerbation of diabetic nephropathy in animals treated with an iSGLT2.(64) This may be indicative of a shift towards fatty acid metabolism, a state where high glucagon/insulin ratio develops, prompting gluconeogenesis, lipolysis and ketogenesis.(94) While this feedback may have positive consequences, a severe switch to lipidic metabolism may induce metabolic acidosis.(94) Metabolic acidosis may be a contributor to progression of kidney disease, and previous reports have shown that metabolic acidosis could be a consequence of iSGLT2 treatment.(94–97) Further reports of gluconeogenic enzyme Pck1 had distinct outcomes, showing either downregulation or absence of significant effect. This diversity of results indicates that SGLT2 blockade may have different outcomes in distinct contexts. Indeed, gluconeogenic pathway activation is a multifactorial process with close correlation to effective cellular glucose uptake.(98,99) This could be particularly important in tubular cells, where SGLT2 inhibition in combination with other factors (*e.g.* peritubular capillaries glucose concentration) may hinder glucose availability.

In the context of glucose uptake, iSGLT2 action lowered cytosolic glucose content in an *in vitro* model of HK2 cells and a CKD model, but failed to do so in diabetic nephropathy models. The lack of effect in diabetic models may be justified by the prevalence of insulin resistance in the untreated groups, that was otherwise reduced in the treated groups. Nevertheless, normalization of glucose metabolism evidenced by reduction in tricarboxylic acid metabolites and glucose metabolites, was reported even in the absence of reduction in cytosolic glucose content. Further exploration is needed to better understand iSGLT2 substances impact in gluconeogenic activation and renal glucose consumption under diverse circumstances. Such evidence might help to mitigate the risks associated with metabolic imbalances caused by iSGLT2 usage.(94,96,97)

4.1.3. Glucose transporters and related signaling pathways

Protein expression of glucose transporters SGLT1, SGLT2, glucose transporter 1 (GLUT1) and glucose transporter 2 (GLUT2) in renal tissue was not changed in any rodent model upon iSGLT2 action. However, it should be noted that the relation between diabetes and SGLT2 upregulation has been previously established in both T2DM humans and T2DM mice, due to exposition to high basolateral glucose levels in proximal tubule cells.(100) The lack of T2DM experimental models reporting SGLT2 protein expression levels in our review limits the validation of this evidence.

4.1.4. Cardiorenal and hemodynamic features

Heart rate mean blood pressure and diastolic blood pressure did not benefit from iSGLT2 treatment in the studies included in our review. Considering heart rate, results are in line with previous clinical trials, where iSGLT2 treatment was associated with cardiovascular and renal protection despite a lack of impact in heart rate changes.(101) Diastolic blood pressure did not match the results from clinical trials. However, this reduction (-1,6 mmHg) was more modest when compared to that of systolic blood pressure (-4,0 mmHg).(101) That contrast may help to comprehend why, for the animal experiments included in our review, both diastolic and mean blood pressure did not reached statistical significant values under SGLT2 blockade. On the other hand, systolic blood pressure was lowered in models of CKD, T1DM and T2DM. This data supports the glucose-independent mechanisms previously reported for iSGLT2 capacity on blood pressure regulation.(102,103)

On the RAAS axis, namely in systemic quantifications, plasmatic renin levels were increased and plasmatic aldosterone unchanged. Such outcomes are in line with previous clinical and pre-clinical data, in which iSGLT2 treatment was associated with RAAS activation, with relevant effects in plasmatic renin upregulation and few relevant changes in plasmatic aldosterone.(104) This has been associated to the feedback of increased urine output and sodium delivery to the juxtaglomerular apparatus, mainly in early stages of iSGLT2 treatment. Nevertheless, despite the apparent iSGLT2 mediated systemic RAAS activation, acceptable blood pressure control is largely achieved.(105)

Urinary and renal RAAS measures had distinct results. Renal cortical concentration of AT1, urinary angiotensinogen and urinary angiotensin II were diminished but urinary aldosterone was not changed by iSGLT2. In previous studies, angiotensinogen has been shown to be locally synthetized in proximal tubular cells, and these cells have also shown to have extensive expression of

AT1.(106,107) Moreover, urinary angiotensinogen has been linked to intrarenal angiotensinogen production.(108) Therefore, iSGLT2 action seems to have a downregulating effect in intrarenal RAAS, contrarily to that of systemic RAAS. Presented evidence emphasizes that the sphere of influence of SGLT2 inhibition in local and systemic RAAS is very likely to be multifaceted. Further studies are encouraged, as such mechanisms could be key players in local and systemic hemodynamic regulation of kidney disease.

4.1.5. Kidney histology and morphological features

In early stages of diabetic nephropathy major structural changes occur, contributing to cortical enlargement and renal hypertrophy, namely tubular thickening and glomerular expansion.(109) It is thought that tubular thickening accounts for most of the increase in kidney weight.(110) However, it is uncertain which of these 2 structural changes occur earlier in diabetic nephropathy progression, or even if other kidney structural changes occur prior to tubular and glomerular enlargement.(109,110) Hyperfiltration is frequently detected alongside discovery of nephromegaly. Although it is still disputed if hyperfiltration precedes kidney enlargement or vice-versa, a model of diabetic rats reported that nephromegaly precedes hyperfiltration.(111) Interestingly, in every experiment included in our review that reported kidney weight reduction or cortical area reduction with iSGLT2 treatment, had associated improvement of kidney function (through either GFR or creatinine clearance). Furthermore, experiments reporting no impact in kidney weight reduction due to iSGTL2 treatment also had no significant improvement in kidney function. This appears to uphold the thesis that nephromegaly precedes hyperfiltration and the ensuing steps of kidney function decline chain.

Despite iSGLT2 ability to restore glomerular hypertrophy, there was no relation between the effect on glomerular hypertrophy and kidney growth. Information regarding iSGLT2 impact on tubular hypertrophy could be useful in establishing a relation between iSGLT2, kidney growth and kidney function decline.

Other glomerular anatomic features were largely ameliorated. Notably, various scoring systems were applied, and improvement was reported in mesangial matrix score, glomerulosclerosis index and glomerular injury score. Also, in a model of CKD, SGLT2 inhibition was able to increase podocyte density as well as α-actinin-4 and β1-Integrin, podocyte adhesion proteins to glomerular basement, indicating that glomerular protection arises irrespective of hyperglycemic status.

In the context of renal circulation, one of the main complications is capillary rarefaction. This complication arises from various sources, such as inflammatory status and injury signals from

adjacent tubular cells.(112) In our review, renal circulation was improved in the few experiments that analyzed these parameters. Renal vascular pressure was reduced in a model of diabetic nephropathy. Periarterial fibrosis, either through direct histologic observation or through NG2 quantification, was reduced in a model of diabetic nephropathy and in a model of CKD. SGLT2 inhibition also increased vascular endothelial growth factor A, an important factor for the maintenance of capillary density. A previous study targeting tubular damage, demonstrated that injury to tubular epithelial cells resulted in tubular degeneration and interstitial capillary loss that later evolved to fibrosis, proteinuria and glomerulosclerosis.(113) In a similar fashion, iSGLT2 mediated reduction in tubular insults seems to be a heavy contributor to these effects, namely in reversing capillary integrity and periarterial fibrosis.

Hypoxia is a logical consequence of decline in renal circulation. Cortical hypoxia was reduced in a model of *db/db* mice, despite medullar hypoxia remaining unchanged. Interestingly, luseogliflozin improved the hemorrhage score registered in a model of CKD. The observed evidence in this area seems to be a down-stream consequence of the previously described reduction in tubular insults and consequent improvement of capillary matrix. This hypothesis could particularly justify the different effects between cortical and medullar hypoxia, as cortical area would benefit the most from reduction in tubular injury.

Finally, renal protein and triglyceride content was reduced upon iSGLT2 treatment. Metabolic profile amelioration, as previously described, and improvement in glomerular filtration are likely the main contributors for those outcomes. On the other hand, calcium oxalate deposition was not ameliorated with iSGLT2 treatment, indicating that eventual benefits on acute compound deposition are less remarkable.

Overall, data gathered in the present review highlight iSGLT2 ability to ameliorate pathological changes in kidney structural features, mainly in models of CKD and diabetic nephropathy.

4.1.6. Kidney function

Waste products cleared exclusively by the kidneys are good indicators of kidney function and in this area, BUN and serum creatinine are the most commonly measured parameters.(114) BUN and serum creatinine were constantly lowered in animals treated with iSGLT2 drugs. SGLT2 inhibition only failed to achieve statistical significance in reducing either of these parameters in shorter experimental models of AKI and experimental models of CKD. Estimation of glomerular filtration followed the same improvement pattern. Firstly, iSGLT2 reduced GFR in animals that experienced hyperfiltration when treatment was absent, including models of diabetic

nephropathy and CKD. Secondly, iSGLT2 decreased creatinine clearance in models of diabetic nephropathy that exhibited hyperfiltration but raised creatinine clearance in experimental models that otherwise experienced decrease filtration rate with privation of treatment. Diabetic nephropathy may develop with an early stage of hyperfiltration followed by a rapid decline in kidney filtration capacity.(111) Also, it is relevant to note that two factors affect filtration rate: individual nephron filtration capacity and the number of functioning glomeruli.(110) Hence, the number of functioning glomeruli might be decreased but global filtration rate may be within normal range or may even be decreased despite individual glomeruli hyperfiltration, justifying the variance of comparative results observed between treated and untreated groups.

Indicators of kidney dysfunction were lowered when iSGLT2 treatment was employed. These parameters more closely represent renal function loss, but once they are present, severe injury has already occurred.(27) Urinary albumin and protein excretion was diminished as evidenced by albuminuria, proteinuria and albumin to creatinine ratio reduction. Conversely, one study reported an increase in albuminuria and albumin to creatinine ratio, indicating a deterioration of kidney function. This particular case was possibly linked to an extreme imbalance in metabolic shift from glucose to lipid metabolism, that ultimately contributed to aggravation of kidney function. Proteinuria was only decreased in models of uninephrectomyzed diabetic animals.

It would be expected that molecules inhibiting glucose reabsorption in nephrons by blocking SGLT2 would continuously increase urine glucose content. However, distinct variations in glucosuria were observed comparing treated and untreated animals. Impact of iSGLT2 on systemic glucose homeostasis helps to justify the spectra of results, as untreated animals with uncontrolled plasmatic glucose levels can achieve higher glucosuria than animals treated with iSGLT2 and controlled plasmatic glucose. This observation can be reinforced by the experiment which reported lower filtered glucose load in the treated group but had no significant differences in urinary glucose among groups. Urine volume displayed variant results, but as urine volume is increased with glucose excretion, it is comprehensible that these two parameters follow similar patterns. Among other components excreted through urine, only urinary sodium excretion was affected by iSGLT2 treatment, as expected due to their mechanisms of action.

Remarkably, there was very strong evidence of glomerular and tubular injury reduction due to SGLT2 blockade, involving models of CKD, T1DM nephropathy and T2DM nephropathy. While urinary excretion of podocalyxin and nephrin were reversed in every experiment, tissue concentrations of nephrin, nestin and synaptopodin were improved, indicating glomerular

protection. Likewise, tissue concentrations of FABP, KIM1 and NAG were reduced and Slc34a1, a marker of tubular integrity, was improved by iSGLT2, beckoning tubular protection. Global kidney injury, assessed by indicators NGAL, TIMP2 and vanin 1, was reduced as attested by reduction of these proteins' expression levels.

iSGLT2 ability to reduce renal injury and improve function was predominantly demonstrated across all considered parameters. Decline in tubular glucotoxicity is likely responsible for the observed effects. How this effect translates to non-diabetic kidney disease remains to be highlighted in pre-clinical studies, as the collected evidence had no data on this field.

4.1.7. Oxidative stress

Markers of oxidative stress have shown remarkable improvements with iSGLT2 treatment. In fact, an outstanding reduction of oxidative stress was seen in every study who focused oxidative state analysis, namely lipid oxidation (MDA reduction), protein oxidation (3NT reduction) and acid nucleic oxidation (8OHdG). In the field of non-enzymatic oxidation, high glucose is a heavy contributor to the imbalance in oxidative state. A constant state of high glucose contributes to lipid oxidation and protein glycation, that in turn can affect critical enzymes and cellular mechanisms.(115) The fact that SGLT2 inhibition so steadily reduced markers of oxidative stress is a great indicator of the potential of iSGLT2 to mitigate oxidative stress mediated injury in the diabetic kidney.

Biologic systems employ endogenous oxidant/antioxidant measures or take advantage of exogenous oxidants/antioxidants to balance oxidative state.(116) Such endogenous measures are, for instance, enzymes responsible for neutralization and production of ROS. Superoxide generator family isoforms Nox2 and Nox4 had their protein expression was reduced in every group of animals receiving iSGLT2. Another enzyme, nitric oxide synthase, had its inducible isoform iNOS reduced by SGLT2 inhibition and its endothelial isoform eNOS induced. Finally, SOD2 and SOD1 levels were increased in SGLT-2 treated diabetic animals

Another important enzymatic process is the glutathione antioxidant system, an important indicator of global red-ox state of an organism.(117) In the data collected for this review, the outcomes where generally indicative of iSGLT2 treatment capacity to cope with oxidative damage. Besides the referred increases in GSH-PX and GSH, the only study reporting absence of statistically significant variations in GSH and GSSG levels, made case to mention an important effect in reducing GSSG concentration and enhancing GSH concentration, bringing both values close to those of healthy animals. Lastly, it should be noted that the aforementioned results in enzymatic

control of oxidative stress are backed up by results such as hydrogen peroxide levels reduction, improvement of TAC and reduction of TOS.

Regarding AGEs related parameters, SGLT2 blockade improved every quantified feature. Diabetic animal models experienced a reduction in AGE-modified proteins and RAGE expression levels, while sRAGE was improved. Also, HMGB1 and RAGE were reduced in HK2 cells, indicating iSGLT2 protection trough inhibition of HMGB1-RAGE-NF-κB signaling pathway. RAGE involvement in diabetic complications progression, such as diabetic nephropathy, has been proved to be halted by preventing AGEs formation.(118) Unfortunately, we could not gather information on oxidative stress mediation by iSGLT2 in CKD or AKI. Hopefully, future endeavors bring useful information in this relation.

4.1.8. Inflammation

Inflammation is a process mediated by cytokines, through a combination of paracrine and autocrine activation pathways, that recruit an immune response with an important protective regulatory role but that can also be a relevant injury effector.(119) Even a low inflammatory state has been hailed as a contributor to progression of diabetic associated complications.(120)In this regard, various cytokines were evaluated in the presently selected investigations. There was a clear relation between iSGLT2 treatment and downregulation of inflammatory cytokines IL1, IL6, CCL2, TNFα and TGFβ, indicating a reduced inflammatory state and inflammatory cell recruitment. Reduction of other inflammatory proteins was also observed upon SGLT2 blockade as demonstrated by COX2 and C-reactive protein expression.

Considering iSGLT2 ability to reduce the expression of cytokines, it's understandable the effect on the evaluated white blood cells. Presence of immune cells in kidney tissue was assessed by evaluation of surface proteins and by histologic visualization. Macrophage infiltration was reduced as represented by reduction in expression of clusters of differentiation CD14, CD11c, CD68 and immunohistochemical data. Other immunity system cells were similarly lowered, as supported by ICAM1 and TLR4 receptors expression reduction (including a model of AKI for the latter), and by the reported histology amelioration of basophilic score and inflammatory cell infiltration score.

4.1.9. Fibrosis

Fibrosis is an excellent indicator of kidney injury, particularly those with chronic and progressive features, like CKD and diabetic nephropathy. Irrespective of underlying disease, kidney fibrosis is the common outcome of chronic kidneys diseases.(121)

Histologic observation revealed a reduction in whole kidney fibrotic area, and this reduction was observed in both cortical fibrosis and medullary fibrosis. Total collagen and individual collagen isoforms where improved in models of diabetic nephropathy and *in vitro* experiments. Likewise, αSMA, fibronectin and F-actin were reduced in animals treated with iSGLT2 substances.

The *in vitro* demonstration that accounts for the downregulation of PDGF-B, THBS1 and TNC (proteins involved in the tubulointerstitial fibrotic process) when canagliflozin and empagliflozin was applied to HK2 cells insulted by TGFβ could provide important clues for iSGLT2 process in fibrosis alleviation. This implies that, at least in a cellular level, iSGLT2 has some protective effect regardless of glucose levels.

It's interesting to notice that multiple parameters of kidney fibrosis were ameliorated in models of AKI, CKD and diabetic nephropathy due to iSGLT2 action. Renal fibrosis can be induced as a consequence of distinct factors, such as inflammation, metabolic imbalances and oxidative stress.(122) The previously observed effects of iSGLT2 in each of these individual areas can help to comprehend the polyvalent ability to reduce fibrosis in distinct renal diseases.

4.1.10. Cellular response to stress

Apoptosis is a mechanism of programmed cell death, important for complex organisms' survival. However, exacerbation of this mechanism has been associated with injury to multiple organs, including the kidney.(123) Various factors, such as hyperglycemia, angiotensin II, AGEs or redox imbalances, can induce a vicious cycle of ROS formation and inflammatory cells and cytokines recruitment. When anti-inflammatory, antioxidant and anti-apoptotic measures are insufficient to counteract this imbalance, the cell activates apoptosis through the intrinsic or extrinsic pathway.(124,125) In this review, we observed a reduction in global apoptosis, as assessed by TUNEL assay, in both models of diabetic nephropathy and CKD.

The mitochondria is a very relevant contributor in apoptosis regulation.(123) In this area, improvement of mitochondrial morphology was achieve by iSGLT2 treatment, as well as reduction of Cytochrome C, both in T2DM models. Furthermore, mitochondrial fusion proteins Mfn2 and Opa1 were also raised in diabetic nephropathy models and in an *in vitro* model insulted by

palmitate. Finally, Bax and Bcl2 regulation of apoptosis was driven into the anti-apoptotic route by iSGLT2 treatment, in both diabetic nephropathy and CKD models, as well as an *in vitro* model.

In diabetic models of nephropathy, various other proteins were successfully downregulated by iSGLT2, such as BIP, Calpain2, CHOP and diverse members of the caspase family, namely Caspase-12, Cleaved caspase-3 and Caspase-7. Lastly, poly-ADP-ribose polymerase (PARP) was also reduced by iSGLT2 in a CKD model and an *in vitro* model insulted by hypoxia. The previous evidence suggests that iSGLT2 mediated apoptosis inhibition is achieved by reducing activation of apoptosis pathways, independent of underlying disease. The previously discussed reduction in inflammation and oxidative stress is the likely cause of this reduction.

Other cellular life cycle regulatory mechanisms were scarcely targeted. Suggestion towards iSGLT2 potential in regulating cell senescence was brought forward by evidence of cyclin-dependent kinase p27 reduction in a model of T1DM.

5. Conclusion

iSGLT2 drugs, through their glucose lowering mechanism of action, induce a shift in metabolic profile and hemodynamic variables thus improving insulin resistance, glycemic levels, blood pressure and overall body composition. However, occasionally, this shift in metabolic profile can trigger a feedback loop responsible for severe imbalances, such as ketoacidosis. Therefore, a proper comprehension of putative factors that contribute to aforementioned outcome is relevant for iSGLT2 safety improvement.

Renal hypertrophy is one of the earlier indicators of renal disease onset and iSGLT2 treatment has shown to be capable to reverse this pathological feature, with consequential impact on aspects of disease progression such as glomerular filtration degradation and tubular injury. Remarkably, every experiment that reported kidney weight reduction with iSGLT2 treatment, also reported normalization of kidney function. These results suggest that delaying functional renal structures damage can be the key step underlying iSGLT2 nephroprotection.

Oxidative stress, inflammation and fibrosis are intertwined processes that contribute to kidney disease progression and undermine nephron function, mainly by glomerulosclerosis and tubulointerstitial fibrosis. Furthermore, with current therapeutic arsenal, the inception of glomerulosclerosis and tubulointerstitial fibrosis carries irreversible injuries that hinder kidney function and morphology, providing a worst prognostic for every physiological and pathological process associated with kidney health. iSGLT2 treatment improved both function and morphological features. Grasping the finetune of iSGLT2 mechanism of action can be of the utmost importance to update the design of more efficient substances and develop better therapeutic strategies related to this class of medicines.

6. References

1. Cho NH, Shaw JE, et al. IDF Diabetes Atlas: Global estimates of diabetes prevalence for 2017 and projections for 2045. *Diabetes Res Clin Pract.* 2018;138:271–81. Available from: doi:10.1016/j.diabres.2018.02.023
2. Olokoba AB, Obateru OA, et al. Type 2 diabetes mellitus: a review of current trends. *Oman Med J.* 2012;27(4):269–73. Available from: doi:10.5001/omj.2012.68
3. World Health Organisation. *Fact sheets, Details, Diabetes*. Available from: https://www.who.int/en/news-room/fact-sheets/detail/diabetes [accessed: 10/27/2019].
4. DeFronzo RA. From the Triumvirate to the Ominous Octet: A New Paradigm for the Treatment of Type 2 Diabetes Mellitus. *Diabetes.* 2009;58(4):773–95. Available from: doi:10.2337/db09-9028
5. Joseph JJ, Echouffo Tcheugui JB, et al. Renin-Angiotensin-Aldosterone System, Glucose Metabolism and Incident Type 2 Diabetes Mellitus: MESA. *J Am Heart Assoc.* 2018;7(17):e009890. Available from: doi:10.1161/JAHA.118.009890
6. Scragg R, Sowers M, et al. Serum 25-Hydroxyvitamin D, Diabetes, and Ethnicity in the Third National Health and Nutrition Examination Survey. *Diabetes Care.* 2004;27(12):2813–8. Available from: doi:10.2337/diacare.27.12.2813
7. Petersen MC, Shulman GI. Mechanisms of Insulin Action and Insulin Resistance. *Physiol Rev.* 2018;98(4):2133–223. Available from: doi:10.1152/physrev.00063.2017
8. Alberti KGMM, Eckel RH, et al. Harmonizing the Metabolic Syndrome A Joint Interim Statement of the International Diabetes Federation Task Force on Epidemiology and Prevention; National Heart, Lung, and Blood Institute; American Heart Association; World Heart Federation; International A. 2009; Available from: doi:10.1161/CIRCULATIONAHA.109.192644
9. Harris MI, Klein R, et al. Onset of NIDDM occurs at Least 4-7 yr Before Clinical Diagnosis. *Diabetes Care.* 1992;15(7):815–9. Available from: doi:10.2337/diacare.15.7.815
10. Spijkerman AMW, Dekker JM, et al. Microvascular Complications at Time of Diagnosis of Type 2 Diabetes Are Similar Among Diabetic Patients Detected by Targeted Screening and Patients Newly Diagnosed in General Practice The Hoorn Screening Study. *Diabetes Care.* 2003;26:2604–2608. Available from: doi:10.2337/diacare.26.9.2604
11. Russell NDF, Cooper ME. 50 years forward: mechanisms of hyperglycaemia-driven diabetic complications. *Diabetologia.* 2015;58(8):1708–14. Available from: doi:10.1007/s00125-015-3600-1
12. Stratton IM. Association of glycaemia with macrovascular and microvascular complications of type 2 diabetes (UKPDS 35): prospective observational study. 2000;321(7258):405–12. Available from: doi:10.1136/bmj.321.7258.405
13. Klein S, Sheard NF, et al. Weight management through lifestyle modification for the prevention and management of type 2 diabetes: rationale and strategies. A statement of the American Diabetes Association, the North American Association for the Study of Obesity, and the American So. *Am J Clin Nutr.* 2004;80(2):257–63. Available from: doi:10.1093/ajcn/80.2.257
14. Davies MJ, D'Alessio DA, et al. Management of Hyperglycemia in Type 2 Diabetes, 2018. A

Consensus Report by the American Diabetes Association (ADA) and the European Association for the Study of Diabetes (EASD). *Diabetes Care.* 2018; Available from: doi:10.2337/DCI18-0033

15. Thrasher J. Pharmacologic Management of Type 2 Diabetes Mellitus: Available Therapies. *Am J Cardiol.* 2017;120(1):S4–16. Available from: doi:10.1016/j.amjcard.2017.05.009

16. Bołdys A, Okopień B. Inhibitors of type 2 sodium glucose co-transporters--a new strategy for diabetes treatment. *Pharmacol Rep.* 2009;61(5):778–84. Available from: doi:10.1016/s1734-1140(09)70133-1

17. Vallon V, Sharma K. Sodium-glucose transport: role in diabetes mellitus and potential clinical implications. *Curr Opin Nephrol Hypertens.* 2010;19(5):425–31. Available from: doi:10.1097/MNH.0b013e32833bec06

18. Bays H. Sodium Glucose Co-transporter Type 2 (SGLT2) Inhibitors: Targeting the Kidney to Improve Glycemic Control in Diabetes Mellitus. 2013; Available from: doi:10.1007/s13300-013-0042-y

19. Wallace MA. Anatomy and Physiology of the Kidney. *AORN J.* 1998;68(5):799–820. Available from: doi:10.1016/S0001-2092(06)62377-6

20. Leslie SW, Sajjad H, et al. *Anatomy, Abdomen and Pelvis, Renal Artery*. Available from: http://www.ncbi.nlm.nih.gov/pubmed/29083626 [accessed: 11/17/2019].

21. Rodriguez F, Cohen F, et al. *Toxicology of the Kidney, 3rd Edition*. Available from: https://www.taylorfrancis.com/books/9780203646991 [accessed: 11/17/2019].

22. Ogobuiro I, Tuma F. *Physiology, Renal*. Available from: http://www.ncbi.nlm.nih.gov/pubmed/30855923 [accessed: 11/02/2019].

23. Basile DP, Anderson MD, et al. Pathophysiology of acute kidney injury. *Compr Physiol.* 2012;2(2):1303–53. Available from: doi:10.1002/cphy.c110041

24. Webster AC, Nagler E V, et al. Chronic Kidney Disease. *Lancet.* 2017;389(10075):1238–52. Available from: doi:10.1016/S0140-6736(16)32064-5

25. Jerums G, Premaratne E, et al. New and old markers of progression of diabetic nephropathy. *Diabetes Res Clin Pract.* 2008;82:S30–7. Available from: doi:10.1016/j.diabres.2008.09.032

26. Piccoli GB, Grassi G, et al. Diabetic Kidney Disease: A Syndrome Rather Than a Single Disease. *Rev Diabet Stud.* 2015;12(1–2):87–109. Available from: doi:10.1900/RDS.2015.12.87

27. Cao Z, Cooper ME. Pathogenesis of diabetic nephropathy. *J Diabetes Investig.* 2011;2(4):243–7. Available from: doi:10.1111/j.2040-1124.2011.00131.x

28. Kanwar YS, Sun L, et al. A glimpse of various pathogenetic mechanisms of diabetic nephropathy. *Annu Rev Pathol.* 2011;6:395–423. Available from: doi:10.1146/annurev.pathol.4.110807.092150

29. Vallon V, Thomson SC. Renal function in diabetic disease models: the tubular system in the pathophysiology of the diabetic kidney. *Annu Rev Physiol.* 2012;74:351–75. Available from: doi:10.1146/annurev-physiol-020911-153333

30. Tan J, Zwi LJ, et al. Presentation, pathology and prognosis of renal disease in type 2 diabetes. *BMJ open diabetes Res care.* 2017;5(1):e000412. Available from:

doi:10.1136/bmjdrc-2017-000412

31. Mohammed-Ali Z, Carlisle RE, et al. Animal Models of Kidney Disease. *In: Animal Models for the Study of Human Disease.* Elsevier; 2017. p. 379–417. Available from: doi:10.1016/B978-0-12-809468-6.00016-4
32. Kong L-L, Wu H, et al. Advances in murine models of diabetic nephropathy. *J Diabetes Res.* 2013;2013:797548. Available from: doi:10.1155/2013/797548
33. Radenković M, Stojanović M, et al. Experimental diabetes induced by alloxan and streptozotocin: The current state of the art. *J Pharmacol Toxicol Methods.* 2016;78:13–31. Available from: doi:10.1016/j.vascn.2015.11.004
34. Chang J-H, Gurley SB. Assessment of Diabetic Nephropathy in the Akita Mouse. *In: Animal Models in Diabetes Research.* Totowa, NJ: Humana Press; 2012. p. 17–29. Available from: doi:10.1007/978-1-62703-068-7_2
35. Sharma K, McCue P, et al. Diabetic kidney disease in the db / db mouse. *Am J Physiol Physiol.* 2003;284(6):F1138–44. Available from: doi:10.1152/ajprenal.00315.2002
36. Clee SM, Nadler ST, et al. Genetic and Genomic Studies of the BTBR *ob/ob* Mouse Model of Type 2 Diabetes. *Am J Ther.* 2005;12(6):491–8. Available from: doi:10.1097/01.mjt.0000178781.89789.25
37. Tomino Y. Lessons From the KK-Ay Mouse, a Spontaneous Animal Model for the Treatment of Human Type 2 Diabetic Nephropathy. *Nephrourol Mon.* 2012;4(3):524–9. Available from: doi:10.5812/numonthly.1954
38. Kawano K, Hirashima T, et al. OLETF (Otsuka Long-Evans Tokushima Fatty) rat: a new NIDDM rat strain. *Diabetes Res Clin Pract.* 1994;24:S317–20. Available from: doi:10.1016/0168-8227(94)90269-0
39. Slyne J, Slattery C, et al. New developments concerning the proximal tubule in diabetic nephropathy: *in vitro* models and mechanisms. *Nephrol Dial Transplant.* 2015;30(suppl 4):iv60–7. Available from: doi:10.1093/ndt/gfv264
40. Afsar B, Elsurer R, et al. The relationship between weight, height and body mass index with hemodynamic parameters is not same in patients with and without chronic kidney disease. *Clin Exp Nephrol.* 2016;20(1):77–86. Available from: doi:10.1007/s10157-015-1136-9
41. Lopez-Giacoman S, Madero M. Biomarkers in chronic kidney disease, from kidney function to kidney damage. *World J Nephrol.* 2015;4(1):57–73. Available from: doi:10.5527/wjn.v4.i1.57
42. Denhez B, Geraldes P. Regulation of Nephrin Phosphorylation in Diabetes and Chronic Kidney Injury. *Protein Rev.* 2017;149–61. Available from: doi:10.1007/5584_2017_62
43. Groma V. Demonstration of collagen type VI and alpha-smooth muscle actin in renal fibrotic injury in man. *Nephrol Dial Transplant.* 1998;13(2):305–12. Available from: doi:10.1093/oxfordjournals.ndt.a027823
44. Street JM, Souza ACP, et al. Automated quantification of renal fibrosis with Sirius Red and polarization contrast microscopy. *Physiol Rep.* 2014;2(7). Available from: doi:10.14814/phy2.12088
45. Agarwal SK, Sethi S, et al. Basics of kidney biopsy: A nephrologist's perspective. *Indian J Nephrol.* 2013;23(4):243–52. Available from: doi:10.4103/0971-4065.114462

46. Matsuyama S, Karim MR, et al. Immunohistochemical analyses of the kinetics and distribution of macrophages in the developing rat kidney. *J Toxicol Pathol.* 2018;31(3):207–12. Available from: doi:10.1293/tox.2018-0002

47. Aydın S, Yanar K, et al. Comparison of oxidative stress biomarkers in renal tissues of d-galactose induced, naturally aged and young rats. *Biogerontology.* 2012;13(3):251–60. Available from: doi:10.1007/s10522-011-9370-3

48. Qi W, Chen X, et al. Transforming growth factor-β 1 differentially mediates fibronectin and inflammatory cytokine expression in kidney tubular cells. *Am J Physiol Physiol.* 2006;291(5):F1070–7. Available from: doi:10.1152/ajprenal.00013.2006

49. Zhan M, Brooks C, et al. Mitochondrial dynamics: regulatory mechanisms and emerging role in renal pathophysiology. *Kidney Int.* 2013;83(4):568–81. Available from: doi:10.1038/ki.2012.441

50. Solini A, Rossi C, et al. Sodium-glucose co-transporter (SGLT)2 and SGLT1 renal expression in patients with type 2 diabetes. *Diabetes, Obes Metab.* 2017;19(9):1289–94. Available from: doi:10.1111/dom.12970

51. Zinman B, Wanner C, et al. Empagliflozin, Cardiovascular Outcomes, and Mortality in Type 2 Diabetes. *N Engl J Med.* 2015;373(22):2117–28. Available from: doi:10.1056/NEJMoa1504720

52. Neal B, Perkovic V, et al. Canagliflozin and Cardiovascular and Renal Events in Type 2 Diabetes. *N Engl J Med.* 2017;377(7):644–57. Available from: doi:10.1056/NEJMoa1611925

53. Pirklbauer M, Schupart R, et al. Unraveling reno-protective effects of SGLT2 inhibition in human proximal tubular cells. *Am J Physiol Physiol.* 2019;316(3):F449–62. Available from: doi:10.1152/ajprenal.00431.2018

54. Panchapakesan U, Pegg K, et al. Effects of SGLT2 Inhibition in Human Kidney Proximal Tubular Cells—Renoprotection in Diabetic Nephropathy? *Stover CM, editor. PLoS One.* 2013;8(2):e54442. Available from: doi:10.1371/journal.pone.0054442

55. Chang Y-K, Choi H, et al. Dapagliflozin, SGLT2 Inhibitor, Attenuates Renal Ischemia-Reperfusion Injury. *Long D, editor. PLoS One.* 2016;11(7):e0158810. Available from: doi:10.1371/journal.pone.0158810

56. Yao D, Wang S, et al. Renoprotection of dapagliflozin in human renal proximal tubular cells via the inhibition of the high mobility group box 1-receptor for advanced glycation end products-nuclear factor-κB signaling pathway. *Mol Med Rep.* 2018;18(4):3625–30. Available from: doi:10.3892/mmr.2018.9393

57. Takagi S, Li J, et al. Ipragliflozin improves mitochondrial abnormalities in renal tubules induced by a high-fat diet. *J Diabetes Investig.* 2018;9(5):1025–32. Available from: doi:10.1111/jdi.12802

58. Zhang Y, Nakano D, et al. A sodium-glucose cotransporter 2 inhibitor attenuates renal capillary injury and fibrosis by a vascular endothelial growth factor–dependent pathway after renal injury in mice. *Kidney Int.* 2018;94(3):524–35. Available from: doi:10.1016/j.kint.2018.05.002

59. Aroor AR, Das NA, et al. Glycemic control by the SGLT2 inhibitor empagliflozin decreases aortic stiffness, renal resistivity index and kidney injury. *Cardiovasc Diabetol.* 2018;17(1):108. Available from: doi:10.1186/s12933-018-0750-8

60. Terami N, Ogawa D, et al. Long-Term Treatment with the Sodium Glucose Cotransporter 2 Inhibitor, Dapagliflozin, Ameliorates Glucose Homeostasis and Diabetic Nephropathy in *db/db* Mice. *Yagihashi S, editor. PLoS One.* 2014;9(6):e100777. Available from: doi:10.1371/journal.pone.0100777

61. Gembardt F, Bartaun C, et al. The SGLT2 inhibitor empagliflozin ameliorates early features of diabetic nephropathy in BTBR ob / ob type 2 diabetic mice with and without hypertension. *Am J Physiol Physiol.* 2014;307(3):F317–25. Available from: doi:10.1152/ajprenal.00145.2014

62. Ishibashi Y, Matsui T, et al. Tofogliflozin, a selective inhibitor of sodium-glucose cotransporter 2, suppresses renal damage in KKAy/Ta mice, obese and type 2 diabetic animals. *Diabetes Vasc Dis Res.* 2016;13(6):438–41. Available from: doi:10.1177/1479164116657304

63. Jaikumkao K, Pongchaidecha A, et al. Dapagliflozin, a sodium-glucose co-transporter-2 inhibitor, slows the progression of renal complications through the suppression of renal inflammation, endoplasmic reticulum stress and apoptosis in prediabetic rats. *Diabetes Obes Metab.* 2018;20(11):2617–26. Available from: doi:10.1111/dom.13441

64. Jia Y, He J, et al. Dapagliflozin Aggravates Renal Injury via Promoting Gluconeogenesis in *db/db* Mice. *Cell Physiol Biochem.* 2018;45(5):1747–58. Available from: doi:10.1159/000487783

65. Kamezaki M, Kusaba T, et al. Comprehensive renoprotective effects of ipragliflozin on early diabetic nephropathy in mice. *Sci Rep.* 2018;8(1):4029. Available from: doi:10.1038/s41598-018-22229-5

66. Kojima N, Williams JM, et al. Renoprotective effects of combined SGLT2 and ACE inhibitor therapy in diabetic Dahl S rats. *Physiol Rep.* 2015;3(7):e12436. Available from: doi:10.14814/phy2.12436

67. Kojima N, Williams JM, et al. Effects of a New SGLT2 Inhibitor, Luseogliflozin, on Diabetic Nephropathy in T2DN Rats. *J Pharmacol Exp Ther.* 2013;345(3):464–72. Available from: doi:10.1124/jpet.113.203869

68. Ma Q, Steiger S, et al. Sodium glucose transporter-2 inhibition has no renoprotective effects on non-diabetic chronic kidney disease. *Physiol Rep.* 2017;5(7):e13228. Available from: doi:10.14814/phy2.13228

69. Nagata T, Fukuzawa T, et al. Tofogliflozin, a novel sodium-glucose co-transporter 2 inhibitor, improves renal and pancreatic function in *db/db* mice. *Br J Pharmacol.* 2013;170(3):519–31. Available from: doi:10.1111/bph.12269

70. Ojima A, Matsui T, et al. Empagliflozin, an Inhibitor of Sodium-Glucose Cotransporter 2 Exerts Anti-Inflammatory and Antifibrotic Effects on Experimental Diabetic Nephropathy Partly by Suppressing AGEs-Receptor Axis. *Horm Metab Res.* 2015;47(09):686–92. Available from: doi:10.1055/s-0034-1395609

71. Oraby MA, El-Yamany MF, et al. Dapagliflozin attenuates early markers of diabetic nephropathy in fructose-streptozotocin-induced diabetes in rats. *Biomed Pharmacother.* 2019;109:910–20. Available from: doi:10.1016/j.biopha.2018.10.100

72. Rajasekeran H, Reich HN, et al. Dapagliflozin in focal segmental glomerulosclerosis: a combined human-rodent pilot study. *Am J Physiol Physiol.* 2018;314(3):F412–22. Available from: doi:10.1152/ajprenal.00445.2017

73. Shin SJ, Chung S, et al. Effect of Sodium-Glucose Co-Transporter 2 Inhibitor, Dapagliflozin, on Renal Renin-Angiotensin System in an Animal Model of Type 2 Diabetes. *Baek K-H, editor. PLoS One.* 2016;11(11):e0165703. Available from: doi:10.1371/journal.pone.0165703

74. Tahara A, Takasu T. Prevention of progression of diabetic nephropathy by the SGLT2 inhibitor ipragliflozin in uninephrectomized type 2 diabetic mice. *Eur J Pharmacol.* 2018;830:68–75. Available from: doi:10.1016/j.ejphar.2018.04.024

75. Tahara A, Takasu T. Effects of the SGLT2 inhibitor ipragliflozin on various diabetic symptoms and progression of overt nephropathy in type 2 diabetic mice. *Naunyn Schmiedebergs Arch Pharmacol.* 2018;391(4):395–406. Available from: doi:10.1007/s00210-018-1469-5

76. Tanaka S, Sugiura Y, et al. Sodium–glucose cotransporter 2 inhibition normalizes glucose metabolism and suppresses oxidative stress in the kidneys of diabetic mice. *Kidney Int.* 2018;94(5):912–25. Available from: doi:10.1016/j.kint.2018.04.025

77. Tang L, Wu Y, et al. Dapagliflozin slows the progression of the renal and liver fibrosis associated with type 2 diabetes. *Am J Physiol Metab.* 2017;313(5):E563–76. Available from: doi:10.1152/ajpendo.00086.2017

78. Vallon V, Gerasimova M, et al. SGLT2 inhibitor empagliflozin reduces renal growth and albuminuria in proportion to hyperglycemia and prevents glomerular hyperfiltration in diabetic Akita mice. *Am J Physiol Physiol.* 2014;306(2):F194–204. Available from: doi:10.1152/ajprenal.00520.2013

79. Wang D, Luo Y, et al. The Sodium-Glucose Cotransporter 2 Inhibitor Dapagliflozin Prevents Renal and Liver Disease in Western Diet Induced Obesity Mice. *Int J Mol Sci.* 2018;19(1):137. Available from: doi:10.3390/ijms19010137

80. Zhang Y, Thai K, et al. Sodium-Glucose Linked Cotransporter-2 Inhibition Does Not Attenuate Disease Progression in the Rat Remnant Kidney Model of Chronic Kidney Disease. *Dussaule J-C, editor. PLoS One.* 2016;11(1):e0144640. Available from: doi:10.1371/journal.pone.0144640

81. Abbas NAT, El. Salem A, et al. Empagliflozin, SGLT2 inhibitor, attenuates renal fibrosis in rats exposed to unilateral ureteric obstruction: potential role of klotho expression. *Naunyn Schmiedebergs Arch Pharmacol.* 2018;391(12):1347–60. Available from: doi:10.1007/s00210-018-1544-y

82. Abdel-Wahab AF, Bamagous GA, et al. Renal protective effect of SGLT2 inhibitor dapagliflozin alone and in combination with irbesartan in a rat model of diabetic nephropathy. *Biomed Pharmacother.* 2018;103:59–66. Available from: doi:10.1016/j.biopha.2018.03.176

83. Cassis P, Locatelli M, et al. SGLT2 inhibitor dapagliflozin limits podocyte damage in proteinuric nondiabetic nephropathy. *JCI Insight.* 2018;3(15). Available from: doi:10.1172/jci.insight.98720

84. Gallo LA, Ward MS, et al. Once daily administration of the SGLT2 inhibitor, empagliflozin, attenuates markers of renal fibrosis without improving albuminuria in diabetic *db/db* mice. *Sci Rep.* 2016;6(1):26428. Available from: doi:10.1038/srep26428

85. Gangadharan Komala M, Gross S, et al. Inhibition of Kidney Proximal Tubular Glucose Reabsorption Does Not Prevent against Diabetic Nephropathy in Type 1 Diabetic eNOS

Knockout Mice. *Ashton N, editor. PLoS One.* 2014;9(11):e108994. Available from: doi:10.1371/journal.pone.0108994

86. Perkovic V, de Zeeuw D, et al. Canagliflozin and renal outcomes in type 2 diabetes: results from the CANVAS Program randomised clinical trials. *lancet Diabetes Endocrinol.* 2018;6(9):691–704. Available from: doi:10.1016/S2213-8587(18)30141-4

87. Fitchett DH. Empagliflozin and Cardio-renal Outcomes in Patients with Type 2 Diabetes and Cardiovascular Disease - Implications for Clinical Practice. *Eur Endocrinol.* 2018;14(2):40–9. Available from: doi:10.17925/EE.2018.14.2.40

88. Mosenzon O, Wiviott SD, et al. Effects of dapagliflozin on development and progression of kidney disease in patients with type 2 diabetes: an analysis from the DECLARE–TIMI 58 randomised trial. *Lancet Diabetes Endocrinol.* 2019;7(8):606–17. Available from: doi:10.1016/S2213-8587(19)30180-9

89. Perkovic V, Jardine MJ, et al. Canagliflozin and Renal Outcomes in Type 2 Diabetes and Nephropathy. *N Engl J Med.* 2019;380(24):2295–306. Available from: doi:10.1056/NEJMoa1811744

90. Cai X, Yang W, et al. The Association Between the Dosage of SGLT2 Inhibitor and Weight Reduction in Type 2 Diabetes Patients: A Meta-Analysis. 2018;26(1):70–80. Available from: doi:10.1002/oby.22066

91. Storgaard H, Gluud LL, et al. Benefits and Harms of Sodium-Glucose Co-Transporter 2 Inhibitors in Patients with Type 2 Diabetes: A Systematic Review and Meta-Analysis. *PLoS One.* 2016;11(11):e0166125. Available from: doi:10.1371/journal.pone.0166125

92. Lee S. Update on SGLT2 Inhibitors-New Data Released at the American Diabetes Association. *Crit Pathw Cardiol.* 2017;16(3):93–5. Available from: doi:10.1097/HPC.0000000000000125

93. List JF, Whaley JM. Glucose dynamics and mechanistic implications of SGLT2 inhibitors in animals and humans. *Kidney Int.* 2011;79:S20–7. Available from: doi:10.1038/ki.2010.512

94. Ferrannini E, Baldi S, et al. Shift to Fatty Substrate Utilization in Response to Sodium–Glucose Cotransporter 2 Inhibition in Subjects Without Diabetes and Patients With Type 2 Diabetes. *Diabetes.* 2016;65(5):1190–5. Available from: doi:10.2337/db15-1356

95. Chen W, Abramowitz MK. Metabolic acidosis and the progression of chronic kidney disease. *BMC Nephrol.* 2014;15:55. Available from: doi:10.1186/1471-2369-15-55

96. Ogawa W, Sakaguchi K. Euglycemic diabetic ketoacidosis induced by SGLT2 inhibitors: possible mechanism and contributing factors. *J Diabetes Investig.* 2016;7(2):135–8. Available from: doi:10.1111/jdi.12401

97. Donnan K, Segar L. SGLT2 inhibitors and metformin: Dual antihyperglycemic therapy and the risk of metabolic acidosis in type 2 diabetes. *Eur J Pharmacol.* 2019;846:23–9. Available from: doi:10.1016/j.ejphar.2019.01.002

98. Kim JH, Ko HY, et al. Effect of dapagliflozin, a sodium-glucose co-transporter-2 inhibitor, on gluconeogenesis in proximal renal tubules. *Diabetes, Obes Metab.* 2020;22(3):373–82. Available from: doi:10.1111/dom.13905

99. Sasaki M, Sasako T, et al. Dual Regulation of Gluconeogenesis by Insulin and Glucose in the Proximal Tubules of the Kidney. *Diabetes.* 2017;66. Available from: doi:10.2337/db16-1602

100. Umino H, Hasegawa K, et al. High Basolateral Glucose Increases Sodium-Glucose

Cotransporter 2 and Reduces Sirtuin-1 in Renal Tubules through Glucose Transporter-2 Detection. *Sci Rep.* 2018;8(1):6791. Available from: doi:10.1038/s41598-018-25054-y

101. Wan N, Rahman A, et al. The Effects of Sodium-Glucose Cotransporter 2 Inhibitors on Sympathetic Nervous Activity. *Front Endocrinol (Lausanne).* 2018;9:421. Available from: doi:10.3389/fendo.2018.00421

102. Filippatos TD, Tsimihodimos V, et al. Mechanisms of blood pressure reduction with sodium-glucose co-transporter 2 (SGLT2) inhibitors. *Expert Opin Pharmacother.* 2016;17(12):1581–3. Available from: doi:10.1080/14656566.2016.1201073

103. Lambers Heerspink HJ, de Zeeuw D, et al. Dapagliflozin a glucose-regulating drug with diuretic properties in subjects with type 2 diabetes. *Diabetes, Obes Metab.* 2013;15(9):853–62. Available from: doi:10.1111/dom.12127

104. Ansary TM, Nakano D, et al. Diuretic Effects of Sodium Glucose Cotransporter 2 Inhibitors and Their Influence on the Renin-Angiotensin System. *Int J Mol Sci.* 2019;20(3):629. Available from: doi:10.3390/ijms20030629

105. Schork A, Saynisch J, et al. Effect of SGLT2 inhibitors on body composition, fluid status and renin–angiotensin–aldosterone system in type 2 diabetes: a prospective study using bioimpedance spectroscopy. *Cardiovasc Diabetol.* 2019;18(1):46. Available from: doi:10.1186/s12933-019-0852-y

106. Kobori H, Harrison-Bernard LM, et al. Enhancement of Angiotensinogen Expression in Angiotensin II–Dependent Hypertension. *Hypertension.* 2001;37(5):1329–35. Available from: doi:10.1161/01.HYP.37.5.1329

107. Harrison-Bernard LM, Navar LG, et al. Immunohistochemical localization of ANG II AT1 receptor in adult rat kidney using a monoclonal antibody. *Am J Physiol Physiol.* 1997;273(1):F170–7. Available from: doi:10.1152/ajprenal.1997.273.1.F170

108. Kobori H, Harrison-Bernard LM, et al. Urinary excretion of angiotensinogen reflects intrarenal angiotensinogen production. *Kidney Int.* 2002;61(2):579–85. Available from: doi:10.1046/j.1523-1755.2002.00155.x

109. Premaratne E, Verma S, et al. The impact of hyperfiltration on the diabetic kidney. *Diabetes Metab.* 2015;41(1):5–17. Available from: doi:10.1016/j.diabet.2014.10.003

110. Trevisan R, Dodesini AR. The Hyperfiltering Kidney in Diabetes. *Nephron.* 2017;136(4):277–80. Available from: doi:10.1159/000448183

111. Bak M, Thomsen K, et al. Renal enlargement precedes renal hyperfiltration in early experimental diabetes in rats. *J Am Soc Nephrol.* 2000;11(7):1287–92. Available from: https://jasn.asnjournals.org/content/11/7/1287.long [accessed: 02/09/2019].

112. Bonventre J V. Can We Target Tubular Damage to Prevent Renal Function Decline in Diabetes? *Semin Nephrol.* 2012;32(5):452–62. Available from: doi:10.1016/j.semnephrol.2012.07.008

113. Grgic I, Campanholle G, et al. Targeted proximal tubule injury triggers interstitial fibrosis and glomerulosclerosis. *Kidney Int.* 2012;82(2):172–83. Available from: doi:10.1038/ki.2012.20

114. Dabla PK. Renal function in diabetic nephropathy. *World J Diabetes.* 2010;1(2):48–56. Available from: doi:10.4239/wjd.v1.i2.48

115. Asmat U, Abad K, et al. Diabetes mellitus and oxidative stress—A concise review. *Saudi*

Pharm J. 2016;24(5):547–53. Available from: doi:10.1016/J.JSPS.2015.03.013

116. Hurrle S, Hsu WH. The etiology of oxidative stress in insulin resistance. *Biomed J.* 2017;40(5):257–62. Available from: doi:10.1016/j.bj.2017.06.007

117. Ceballos-Picot I, Witko-Sarsat V, et al. Glutathione antioxidant system as a marker of oxidative stress in chronic renal failure. *Free Radic Biol Med.* 1996;21(6):845–53. Available from: doi:10.1016/0891-5849(96)00233-x

118. Sakurai S, Yonekura H, et al. The AGE-RAGE System and Diabetic Nephropathy. *J Am Soc Nephrol.* 2003;14(suppl 3):S259–63. Available from: doi:10.1097/01.ASN.0000077414.59717.74

119. Aldhahi W, Hamdy O. Adipokines, inflammation, and the endothelium in diabetes. *Curr Diab Rep.* 2003;3(4):293–8. Available from: doi:10.1007/s11892-003-0020-2

120. Pickup JC. Inflammation and Activated Innate Immunity in the Pathogenesis of Type 2 Diabetes. *Diabetes Care.* 2004;27(3):813–23. Available from: doi:10.2337/diacare.27.3.813

121. Kanasaki K, Taduri G, et al. Diabetic nephropathy: the role of inflammation in fibroblast activation and kidney fibrosis. *Front Endocrinol (Lausanne).* 2013;4:7. Available from: doi:10.3389/fendo.2013.00007

122. Meran S, Steadman R. Fibroblasts and myofibroblasts in renal fibrosis. *Int J Exp Pathol.* 2011;92(3):158–67. Available from: doi:10.1111/j.1365-2613.2011.00764.x

123. Ortiz A, Lorz C, et al. Contribution of apoptotic cell death to renal injury. *J Cell Mol Med.* 2001;5(1):18–32. Available from: doi:10.1111/j.1582-4934.2001.tb00135.x

124. Wagener F, Dekker D, et al. The role of reactive oxygen species in apoptosis of the diabetic kidney. *Apoptosis.* 2009;14(12):1451–8. Available from: doi:10.1007/s10495-009-0359-1

125. Ramseyer VD, Garvin JL. Tumor necrosis factor-α: regulation of renal function and blood pressure. *Am J Physiol Renal Physiol.* 2013;304(10):F1231-42. Available from: doi:10.1152/ajprenal.00557.2012